ChemSusChem

Tuning thiophene-based phenothiazines for stable photocatalytic H2 production

--Manuscript Draft--

Manuscript Number:	
Article Type:	Full Paper
Corresponding Author:	Paolo Fornasiero Universita degli Studi di Triestes Trieste, ITALY
Corresponding Author E-Mail:	pfornasiero@units.it
Other Authors:	Bianca Cecconi
	Norberto Manfredi
	Riccardo Ruffo
	Tiziano Montini
	ISMAEL ROMERO OCAÑA
	Alessandro Abbotto
Keywords:	hydrogen production photocatalysis dyes stability visible light solar cells
Manuscript Classifications:	Catalysis; Photocatalysis; Renewable hydrogen; Water splitting
Suggested Reviewers:	Davide Bonifazi, Prof. Dr. Universite de Namur davide.bonifazi@unamur.be Expert of organic chemistry - sustainable chemistry - functional hierachical materials
	Vladimiro dal Santo, Dr. Consiglio Nazionale delle Ricerche v.dalsanto@istm.cnr.it expert of hydrogen photocatalytic production.
	Kazuhiro Takanabe, Prof.Dr. King Abdullah University of Science and Technology kazuhiro.takanabe@kaust.edu.sa Expert in photocatalysis and hydrogen production
	Habdul Hameed, Prof.Dr. King Abdulaziz University hameedch@yahoo.com Expert in photocatalysis
	Miguel Banares, Dr. Consejo Superior de Investigaciones Cientificas banares@icp.csic.es Expert in material science, spectroscopy and photocatalysis
	Marcella Bonchio, Prof. Universita degli Studi di Padova marcella.bonchio@unipd.it expert of organic chemistry - materials for photocatalytic water splitting
Opposed Reviewers:	
Abstract:	Dibranched D-(π-A)2 dyes, where D is a phenothiazine donor core, A is an acceptor-anchoring cyanoacrylic group, and π are mono- and polycyclic simple and fused thiophene derivatives, have been tested as photosensitizers in the photocatalytic production of hydrogen, in combination with a Pt/TiO2 catalyst; dyes were investigated

	in their optical and electrochemical properties, showing that the proper design of the thiophene-based π-spacer afforded enhanced optical properties. In the hydrogen production over 20 h the new thiophene-based sensitizers revealed improved stability after longer irradiation times and enhanced performances, in terms of hydrogen production rates and Light-to-Fuel efficiencies, after an initial activation period, which were for the first time associated to enhanced stability under photocatalytic production of hydrogen and the absence of critical dye degradation.
Author Comments:	To Guido Kemeling; Editor-in-Chief of ChemSusChem Dear Editor, We are pleased to submit our manuscript titled "Tuning thiophene-based phenothiazines for stable photocatalytic H2 production" by Bianca Cecconi, Norberto Manfredi, Riccardo Ruffo, Tiziano Montini, Ismael Romero-Ocaña, Paolo Fornasiero* and Alessandro Abbotto* be considered for publication in ChemSusChem as a full paper. This work presents a detailed investigation of a series of organic dyes as sensitizers for - photocatalytic hydrogen production. In this context, we studied molecular di-branched architectures based on a phenothiazine core, as a donor group, and a cyanoacrylic moiety, as an acceptor-anchoring group. We systematically varied the thiophene-based p spacer using mono- and bicyclic, simple and fused, heteroaromatic rings. The new class of dyes has been investigated in their optical and electrochemical properties, and then used as sensitizers both in DSSC and in the photocatalytic production of hydrogen in conjunction with Pt/TiO2. The latter was completed with a detailed morphological investigation of the Pt/TiO2 catalytic centre, to which the dyes have been anchored through their cyanoacrylic moieties. The study clearly demonstrated the influence of the thiophene based spacers on molecular properties and device efficiencies. The optical properties were significantly enhanced both in qualitative and quantitative terms, with strong increase of the molar absorptivity. Remarkably, we show not only promising visible light hydrogen production, but, more importantly, improved stability with respect to reference materials. We believe that these findings can contribute to a rational and viable development of active and stable materials for sustainable hydrogen photoproduction. Therefore, we hope you will agree that this work has the novelty and the general interest to meet the high standards of your journal. Looking forward having the opportunity to reply to the referees comments Best regards, Alessandro Abbotto and Paolo Fornasiero
Section/Category:	
Additional Information:	
Question	**Response**
Dedication	
Submitted solely to this journal?	Yes
Has there been a previous version?	No

Tuning thiophene-based phenothiazines for stable photocatalytic H_2 production

Bianca Cecconi,[a] Norberto Manfredi,[a] Riccardo Ruffo,[a] Tiziano Montini,[b] Ismael Romero Ocaña,[b] Paolo Fornasiero [b]* and Alessandro Abbotto [a]*

Abstract: Dibranched D-(π-A)$_2$ dyes, where D is a phenothiazine donor core, A is an acceptor-anchoring cyanoacrylic group, and π are mono- and polycyclic simple and fused thiophene derivatives, have been tested as photosensitizers in the photocatalytic production of hydrogen, in combination with a Pt/TiO$_2$ catalyst; dyes were investigated in their optical and electrochemical properties, showing that the proper design of the thiophene-based π-spacer afforded enhanced optical properties. In the hydrogen production over 20 h, the new thiophene-based sensitizers revealed improved stability after longer irradiation times and enhanced performances, in terms of hydrogen production rates and Light-to-Fuel efficiencies, after an initial activation period, which were for the first time associated to enhanced stability under photocatalytic production of hydrogen and the absence of critical dye degradation.

Introduction

Solar energy is considered the most powerful renewable source of energy.[1] Electric energy and fuels play essential roles for societal needs and both can be covered by Sun as a primary green and renewable source.[2] Photovoltaic (PV) technologies are able to transform solar radiation into electric currents; amongst them, dye-sensitized solar cells (DSSC), introduced by Graetzel and O'Regan in 1991,[3] play today an increasing prominent role.[4] In the case of solar fuels, solar radiation is converted to chemical energy of bonds in molecules. Hydrogen is particularly attractive as a fuel, since it has no carbon footprint when it is burnt to water and can be obtained through water splitting from an abundant and clean source. Unfortunately, water splitting is an up-hill and kinetically hindered process; the electromagnetic radiation can supply the energy needed to overcome ΔG only if a suitable catalyst is used to reduce the kinetic overpotential.

Fujishima and Honda first introduced in 1972 the use of titanium dioxide as a semiconductor, loaded with platinum nanoparticles on the surface as catalysts, to split water molecules using light.[5] The efficiency of such a system is mainly associated to the fact that only a narrow portion of the sunlight, the ultraviolet region, is able to promote an electron into the conduction band (CB) of TiO$_2$ and to the fast electron-hole recombination process. Indeed, the minimum energy demand for water splitting, 1.23 eV at pH = 0 (corresponding to the near-IR region around 1000 nm), is much lower than the energy band gap in TiO$_2$ (3.0 – 3.2 eV depending on the polymorph, corresponding to a photon with λ ~ 387 – 413 nm). Nevertheless, TiO$_2$ has CB position suitable for proton reduction and remains a very attractive material due to its abundance, relatively low cost, stability against photo-corrosion and no toxicity in form of paste or thin films.[6] Amongst the solutions to improve efficiency of these systems, the introduction of a sensitizer to extend the absorbed portion of solar spectrum is a challenging option.[7] The working mechanism quite closely reminds that of natural photosynthesis, that is the reason why such technologies can be included in the group of the artificial photosynthetic methods.[8] In such an artificial leaf, solar radiation is absorbed by a dye sensitizer D, which is promoted to its excited state D* through a HOMO-LUMO transition. Then, the electron in the dye LUMO is injected to the CB of TiO$_2$ on the surface of which Pt(0) is present and acts as an electron trap. Platinum is able to transfer two electrons to two protons to afford one molecule of H_2. After electron injection, D* has been converted to its radical cation $D^{\cdot+}$, which is then regenerated back to D. In a complete water splitting system the electrons for dye regeneration come from water oxidation to oxygen. If attention is focused only on water reduction to hydrogen, as in our case, a sacrificial electron donor (S) is commonly used, so that the reduction semi-reaction could be the rate-determining step of the whole process.

In this study we focused our attention on the role of the sensitizer D, which plays a central role both in DSSC and in H_2 photo-production being the first direct interface with the solar radiation. In contrast with the huge literature on DSSC sensitizers,[9,10] few articles have studied the role of the dyes in the photocatalytic production of hydrogen. In the latter case the most important families of dyes are the same as in DSSC technology, mostly including organometallic molecules such as ruthenium complexes,[11,12] porphyrins or phtalocyanines inspired by chlorophyll complex.[13] Metal-free organic sensitizers have been gaining an increasing role in the scientific literature of hydrogen production,[14–16] with record DSSC power conversion efficiencies (PCE) exceeding 12%.[17–19] These dyes carry important advantages over metal complexes such as easier and cheaper synthesis and purification, larger structural variety, and wider tunability of optical and energetic properties, which are fundamental to optimize the corresponding solar devices.[20–23] Triggered by the some recent studies on phenothiazines (PTZ) derivatives as DSSC sensitizers [24–27] and by their first uses as light harvesters in the photo-driven production of hydrogen,[28] we decided to systematically investigate this promising class of

[a] Dr. Bianca Cecconi, Dr. Norberto Manfredi, Prof. Riccardo Ruffo and Prof. Alessandro Abbotto
Department of Materials Science, Solar Energy Research Center MIB-SOLAR and INSTM Milano-Bicocca Research Unit
University of Milano-Bicocca,
Via Cozzi 55, I-20125, Milano, Italy
E-mail: alessandro.abbotto@unimib.it
[b] Dr. Tiziano Montini, Dr. Ismael Romero-Ocana and Prof. Paolo Fornasiero
Department of Chemical and Pharmaceutical Sciences; ICCOM-CNR Trieste Research Unit and INSTM Trieste Research Unit
University of Trieste
Via L.Giorgieri 1, I-34127 Trieste, Italy
E-mail: pfornasiero@units.it

Supporting information for this article is given via a link at the end of the document.((Please delete this text if not appropriate))

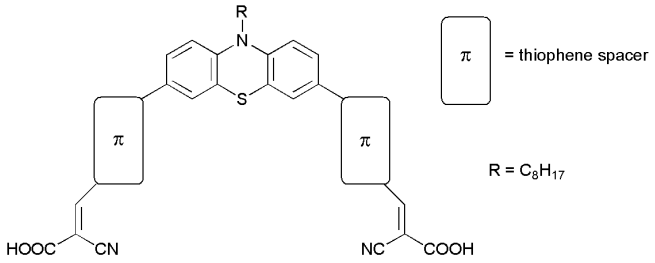

Fig. 1: Class of thiophene-based phenothiazines investigated in this work.

dyes by designing a series of organic sensitizers containing the phenothiazine core as a donor scaffolds in donor-π-acceptor molecules. Interestingly, a very recent report on a class of benzo[b]phenothiazines confirms the increasing relevance of dye-sensitized hydrogen production using organic dyes and phenothiazine derivatives.[29] The phenothiazine core carries peculiar features associated to its non-planar butterfly conformation along the S-N axis. Such arrangement avoids fully planar geometries, which could be detrimental by promoting self-quenching molecular aggregates on the TiO_2 surface. Moreover, the phenothiazine structure contains two symmetric benzene rings which can be conveniently functionalized allowing the design of symmetric di-branched dyes, a recently important class of photosensitizers endowed with higher anchoring stability and electron injection efficiency, improved optical properties, and enhanced device stability which was introduced by us in the DSSC field of investigation and later used by many research groups.[27,30–33] Lastly, the nitrogen atom of the central core of the phenothiazine groups can be conveniently functionalized with alkyl or aryl groups of different chemical nature, in order to provide a further derivatization site able to induce additional properties such as proper solubility in specific media (with particular attention to water) or affinity to bio-inspired molecules. In order to systematically investigate this class of molecules, here we have focused our attention on the effect of the π-spacer group. In particular, thiophene rings have been widely used in materials science due to their peculiar structural and electronic properties.[34] Thiophene is a π-excessive heteroaromatic five-membered ring with a lower resonance energy than benzene, [35] thus facilitating charge transfer between the donor and the acceptor core of the organic dyes. For these reasons thiophene-based spacers have been commonly applied in the design of dyes for solar applications.[20–23,36] We have here exploited different mono-, poly-, and fused polycyclic thiophene-based groups as π-spacers between the phenothiazine donor core and the acceptor/anchoring groups based on cyanoacrylic acid (**Error! Reference source not found.**). As a reference system the previously investigated dye **PTZ1** (named P3 in Ref. [28]) has been included in our work, also because the hydrophobic octyl chain is supposed to raise detrimental charge recombination lifetimes.[28]

Besides paying attention to harvesting visible light, we aimed at exploring the new dyes to overcome the problem of photo-induced degradation of the sensitizers. In particular, we have noticed that most of the reported studies on dye-sensitized production of hydrogen, with rare exceptions,[29] involve relatively short irradiation times (typically around 5 h).[13–16,28,37,38] Such short irradiation periods limit the significance of these studies for realistic applications, not giving a true image of the photocatalytic activity of the dye-sensitized catalyst in the long term. In addition, to the best of our knowledge, no dye photo-degradation studies have been reported so far, though there are clear indications that hydrogen production rate decreases with time for these systems.[28,29]

The new dyes have been characterized in their optical and electrochemical properties and, in combination with TiO_2 and other proper components, investigated as photosensitizers in the photocatalytic H_2 production over 20 h irradiation times. Their activity as sensitizers in DSSC has been also tested. We examined the effect of the molecular design, namely that of the thiophene-based π spacer, on the efficiency of H_2. In particular, remarkably stable photocatalytic activity was observed with an H_2 evolution rate up to 250 μmol g^{-1} h^{-1}, and turnover number (TON) up to 75, making this class of compound particularly promising for solar-based devices. The highest efficiency of one of these dyes over long irradiation times was clearly associated to its higher stability under irradiation, in contrast with other previously reported dyes and with **PTZ1**, used as representative reference literature system in this work, which is strongly unstable under the same experimental conditions.

Results and Discussion

Design and synthesis

The new phenothiazines **PTZ2**-**6** (Fig. 2) have been designed and synthesized. Phenothiazines **PTZ2-6** differ in their thiophene-based π-spacers. The selection of the simple thiophene in **PTZ2** was made to improve optical properties of the dye by both red-shifted and more intense. With the same target in mind **PTZ3** and **PTZ4** have been designed where somewhat more sophisticated heteroaromatic cores have been employed to further modulate optical and electronic characteristics.

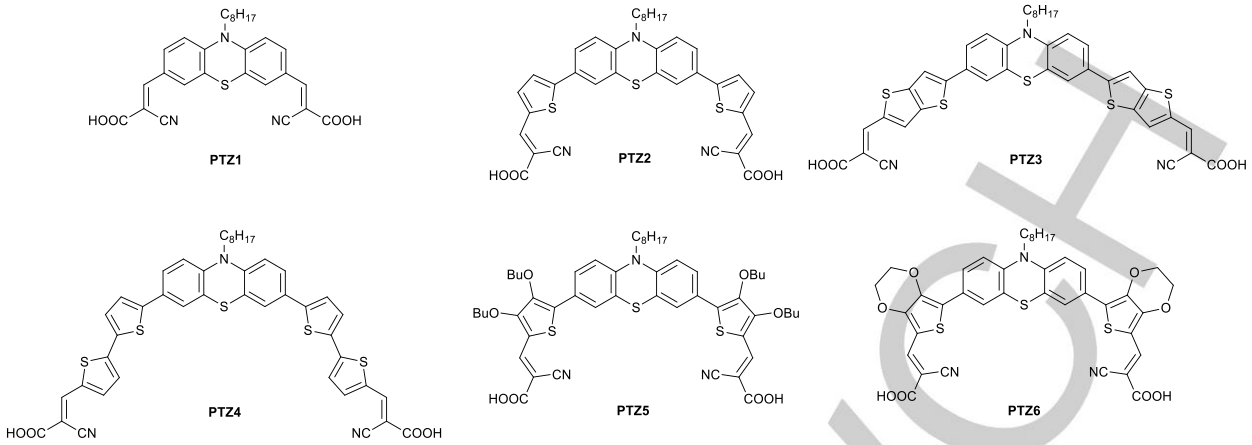

Fig. 2: Structure of the investigated dyes.

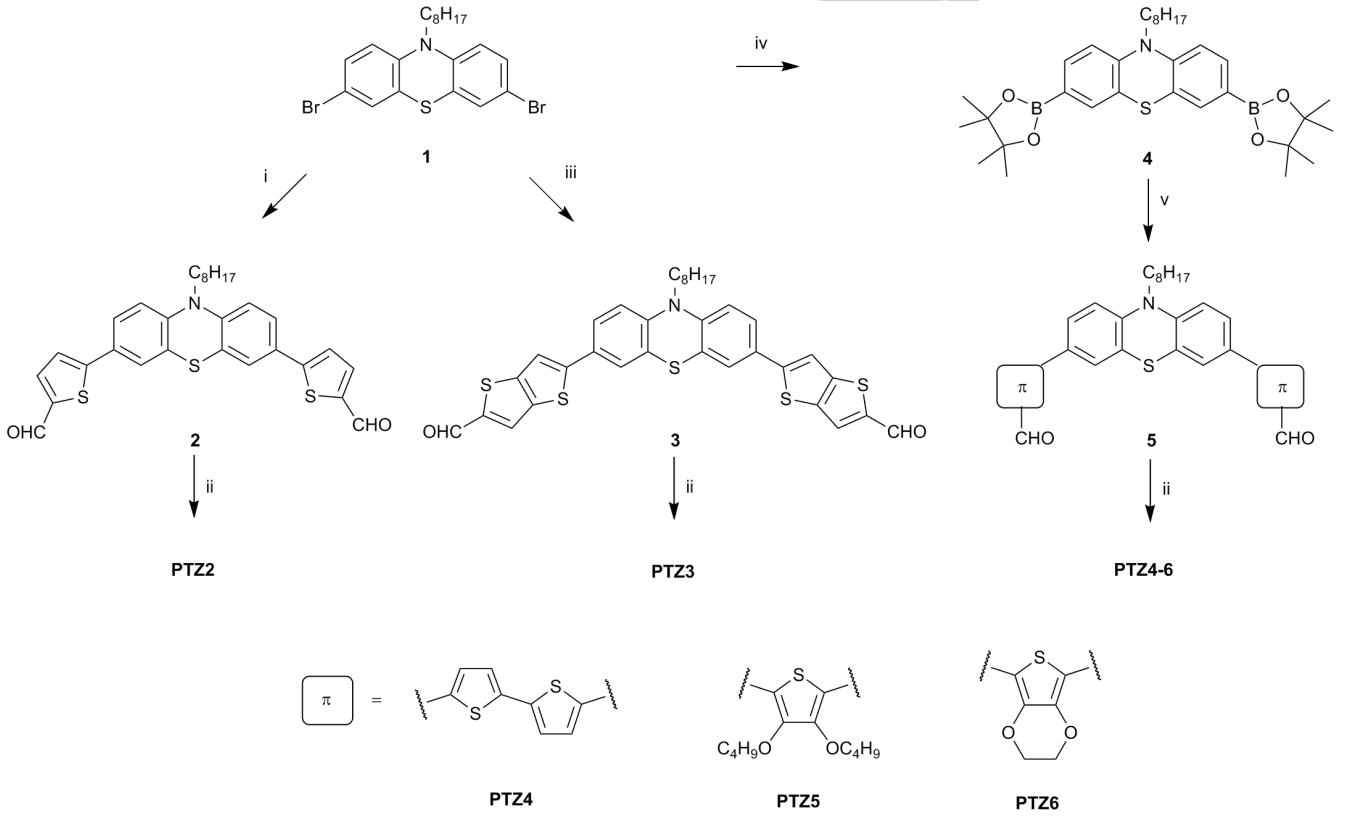

Scheme 1: Synthetic routes for **PTZ2-6**. Reagents and conditions: (i) 5-Formyl-2-thienylboronic acid, $Pd(dppf)Cl_2 \cdot CH_2Cl_2$ [dppf = 1,1′-bis(diphenylphosphino)ferrocene], K_2CO_3, DME/MeOH, microwave 90 °C, 90 min; (ii) cyanoacetic acid, piperidine, $CHCl_3$, 80 °C, 5 h; (iii) a. 4,4,5,5-tetramethyl-2-(thieno[3,2-b]thiophen-2-yl)-1,3,2-dioxaborolane, $Pd(dppf)Cl_2 \cdot CH_2Cl_2$, K_2CO_3, DME/MeOH, microwave 90 °C, 90 min, b. $POCl_3$, DMF, -5 °C to 100 °C, 8h; (iv) a. BuLi, THF, -78 °C, 60 min, b. 2-isopropoxy-4,4,5,5-tetramethyl-1,3,2-dioxaborolane, r.t., 15 h; (v) 5'-bromo-(2,2'-bithiophene)-5-carbaldehyde (**PTZ4**), or 5-bromo-3,4-dibutoxythiophene-2-carbaldehyde(**PTZ5**), or 7-bromo-2,3-dihydrothieno[3,4-b][1,4]dioxine-5-carbaldehyde (**PTZ6**), $Pd(dppf)Cl_2 \cdot CH_2Cl_2$, K_2CO_3, microwave, 90 °C, 90 min.

PTZ5 was prepared both to study the influence of electronrich alkoxy functionalities in the electronic communication between the dye and TiO_2 surface, and to limit dye aggregation thanks to the four butyl chains, that should prevent π-stacking processes. Finally, the 3,4-ethylenedioxythiophene (EDOT) derivative **PTZ6** was synthetized to study the net electronic role of the alkoxy groups without any steric effect as in **PTZ5**. The overall synthetic approach for **PTZ2-6** is depicted in Scheme 1

Dye **PTZ1** has been synthetized according to literature methods starting from commercial 10*H*-phenothiazine. Alkylation at nitrogen was carried out with NaH as a base and 1-bromooctane as the alkylating agent followed by a Vilsmeier-Haack formylation of the aromatic core and Knoevenagel condensation with cyanoacetic acid.[28] Bromination of 10-octyl-10*H*-phenothiazine with NBS in classical conditions gave very low yields (~30 %); thus bromine in acetic acid was preferred (up to 95 % of yield) to synthetize molecule **1**.[39,40] The Suzuki-Miyaura cross coupling reaction, since using boron derivatives is more sustainable than the alternative Stille reaction, was preferred to insert the thiophene-based spacer.[41] Two alternative strategies were used, according to the availability of precursors. The bromo-derivative **1** was coupled to 2-thiophene-aldehyde-5-boronic acid and 4,4,5,5-tetramethyl-2-(thieno[3,2-b]thiophen-2-yl)-1,3,2-dioxaborolane [42] for the synthesis of **PTZ2** and **PTZ3**, respectively. A Vilsmeier-Haack formylation on the thieno[3,2-b]thiophene derivative allowed to isolate molecule **3**. In the case of **PTZ4-6**, for which the bromo-derivatives of the corresponding π-spacers were more readily available, the boronic functionality was placed on phenothiazine core through halogen-metal exchange by *n*-BuLi and subsequent quenching by 2-isopropoxy-4,4,5,5-tetramethyl-1,3,2-dioxaborolane to give the intermediate **4**. The π-precursors for **PTZ4-6** were synthetized according to reported methods in the case of bithienyl [43] and EDOT.[44] To synthetize 5-bromo-3,4-dibutoxythiophene-2-carbaldehyde, similar conditions as that for the EDOT derivative were chosen. 3,4-Dimethoxythiophene was treated with PTSA and butanol to insert the butyl chains [45,46] followed by formylation and bromination with NBS allowed to afford the desired intermediate. Boronic ester **4** was then allowed to react with the corresponding bromo-derivatives under microwave assisted Suzuki-Miyaura cross coupling conditions to isolate carbaldehyde precursors of **PTZ4-6** in comparable yields. Final Knoevenagel condensation with cyanoacetic acid in basic conditions afforded **PTZ2-6** in good yields.

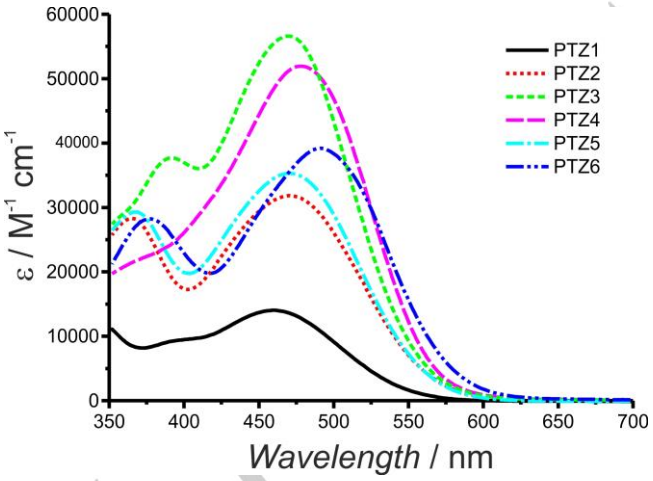

Fig. 3: Absorption spectra of dyes **PTZ1-6** in THF.

Optical and Electrochemical characterization

Optical characterization of dyes **PTZ1-6** was performed in 10^{-5} M THF solution. Absorption spectra normalized to molar extinction coefficients are shown in Fig. 3. All the dyes showed a classical pattern, with an intense absorption band in the Vis region attributed to the intramolecular donor to acceptor charge-transfer transition. Validating the target of this work, the introduction of thienyl π-spacers led to a substantial qualitative and/or quantitative improvement of the optical properties of **PTZ2-6** compared to reference **PTZ1**. Moreover an additional band at higher energies, likely attributed to the local thiophene transitions, is present in the thienyl dyes **PTZ2-6**. The introduction of more structured thiophene-based π-cores resulted to substantial bathochromic and/or hyperchromic effects, thus allowing a more efficient photon harvesting. Such important property is compatible with the use of thinner nanocrystalline films as those required by solid-state devices and in solid-state DSSC.[47,48] It is worth noting that even the introduction of a single thiophene ring in the π-framework afforded a molar extinction coefficient twice as large as in **PTZ1** (from 13700 to 34000 M^{-1} cm^{-1} in **PTZ2**) and a 11-nm red-shifting. The use of spacers with longer conjugation paths confirmed this optical trend allowing us to achieve molar absorptivities up to 60000 $M^{-1}cm^{-1}$ as in **PTZ3** and **PTZ4**, that is more than four times larger than in the reference dye, and, in some cases, absorption peaks at significantly longer wavelengths. In the case of **PTZ3** the introduction of the more π-extended thienothiophene spacer compared to simple thiophene in **PTZ2** was not associated to a bathochromic effect but a substantial hyperchromic effect, with a peak molar absorptivity almost twice as larger than that of the thiophene derivative. A different behavior is recorded for the 3,4-alkoxythienyl derivatives **PTZ5** and **PTZ6** where molar absorptivities are ultimately comparable to that of **PTZ2**, though the presence of the auxochrome groups further shifted the absorption maximum to longer wavelength, reaching a top value of 490 nm for **PTZ6**, to be compared with 460 nm in **PTZ1**. In summary, the introduction of the thiophene-based spacers in **PTZ2-PTZ6** resulted in either significantly red-shifted absorption peaks or enhanced molar absorptivities or a combination of the two effects. Optical bandgaps were calculated by means of the Tauc plots [49] (Fig. S1) and listed in Table 1 together with their main optical parameters. The dyes have very low emission intensity and were not considered reliable enough to calculate zeroth-zeroth energies from the intercept with the normalized absorption spectra. In fact, the shape of the emission spectra is rather broad compared to the absorption bands, likely due to aggregation and intermolecular energy exchange reasons.

Saturated solutions of **PTZ1-6** in CH_2Cl_2 were used for the electrochemical characterization by dissolving each derivate in the supporting electrolyte (0.1 M $TBAClO_4$). The cyclic voltammetry (CV) study (Fig. 4a) showed a quasi-reversible behavior at oxidative potentials (potential > 0 V) and several irreversible reduction waves at the lowest potentials (potential < -1.0 V) for all the dyes. In this latter potential region the main source of current raising was due to the electrolyte

Table 1: Optical characterization of dye **PTZ1-6** in 10^{-5} M THF solution.

Dye	λ_{max} (nm)	ε ($M^{-1}cm^{-1}$)	λ_{onset} (nm)	λ_{em} (nm)	E_{gap}^{opt} (eV)
PTZ1	460	13700 ± 300	590	613	2.10
PTZ2	471	34000 ± 1800	605	654	2.05
PTZ3	470	57800 ± 2900	596	605	2.08
PTZ4	478	56200 ± 2200	598	583	2.07
PTZ5	477	35400 ± 1300	613	598	2.02
PTZ6	490	39200 ± 600	617	654	2.01

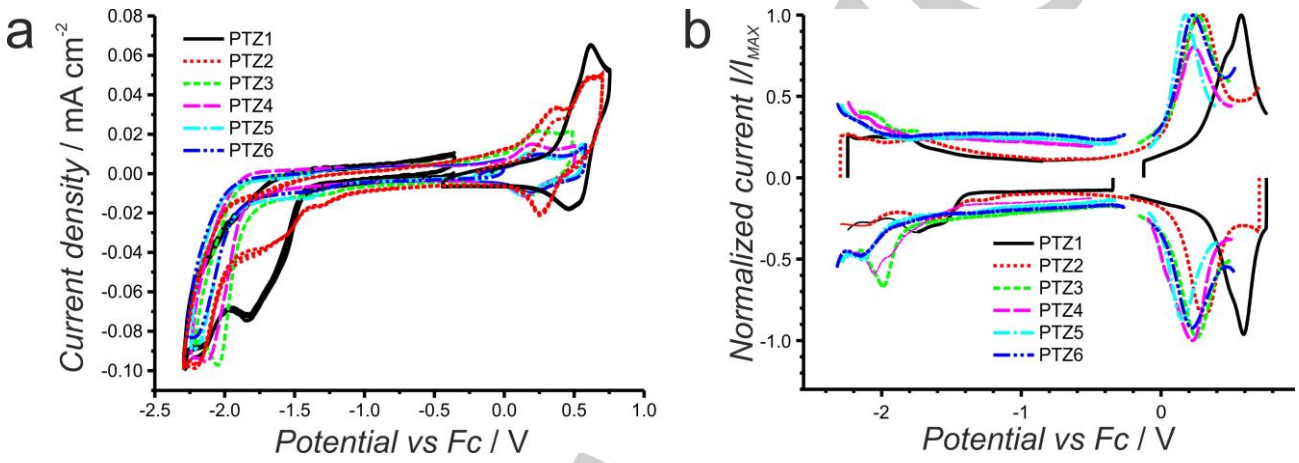

Fig. 4: a) CV traces for PTZ dyes in solution; b) DPV traces for PTZ dyes in solution.

Table 2: Electrochemical characterization of PTZ dyes.[a]

Sample	E^{ox}(V) ± 5 mV	HOMO (eV) ± 50 meV	E^{red} (V) ± 5 mV	LUMO (eV) ± 50 meV
PTZ1	0.39	−5.62	-	−3.52[b]
PTZ2	0.15	−5.38	-	−3.33[b]
PTZ3	0.26	−5.49	−1.99	−3.25
PTZ4	0.27	−5.50	−2.06	−3.17
PTZ5	0.16	−5.39	−2.15	−3.08
PTZ6	0.22	−5.45	−2.16	−3.07

[a] All potentials are reported vs. Fc/Fc^+, and the HOMO and LUMO energies are derived from the electrochemical data based on the assumption that the Fc/Fc^+ redox couple is 5.23 eV relative to a vacuum, using a potential value of 4.6 ± 0.2 eV for NHE vs vacuum [50] and 0.63 eV for Fc/Fc^+ vs NHE.[51] [b] Calculated from electrochemical HOMO energies and optical bandgap.

decomposition. Differential pulse voltammetry (DPV) was preferred for the accurate estimation of the oxidation (E^{ox}) and reduction (E^{red}) potentials and HOMO/LUMO energy levels (Fig. 4b and Table 2). HOMO/LUMO energies are pictorially depicted in Fig. 5 relative to the conduction band level of TiO_2.[52]

All the oxidative processes seem to be constituted by two different waves; the first wave is a shoulder in the case of **PTZ1**. By using DPV the decomposition effect of the electrolyte is minimized and the waves can be more accurately attributed to the investigated molecules. The oxidation potentials of the molecules are similar to each other, as expected for the presence of the same phenothiazine donor core, whereas differences are recorded in their properties at cathodic potentials. All of the thiophene-substituted dyes were found easier to

oxidize than **PTZ1** (lower oxidation potential) by 120 to 240 mV, in agreement with the donor character of the thiophene ring.[53] No substantial differences were found within the thiophene derivatives **PTZ2-PTZ6**, with oxidation potentials being within a range of 120 mV, in agreement with literature data on similar compounds.[24–27] This suggests that the presence of different thiophene spacers and ring substituents did not significantly affect the oxidation potential, and thus the HOMO energy level, of the corresponding dyes. This is in agreement with the spacer character, rather than a donor nature represented by the phenothiazine core, of the thiophene moieties in the donor-π-acceptor dyes. However, we note that the bis-alkoxythiophene derivative **PTZ5**, carrying two electronrich substituents on each thiophene ring, is amongst the most easily oxidized dyes. Two reduction waves were recorded for **PTZ1** and **PTZ2**, which are ascribed to the reductive chemisorption of the acidic protons onto the electrode surface and to the electron injection in the LUMO orbital. The observation that a simple washing step is not enough to detach the dye from the electrode suggested that a strong interaction between the molecules and the glassy carbon surface, after the reductive step, takes place. Due to the multi-wave profile of the reduction processes LUMO energies were not evaluated for **PTZ1** and **PTZ2**. In these cases the LUMO was evaluated from the corresponding HOMO energies and optical bandgaps. The cathodic electrochemistry of **PTZ3-6** molecules is somewhat more regular and the current peak positions were used to calculate their LUMO energy values. As can be seen from Fig. 5 all of the LUMO energies of the new thiophene-based dyes were higher than that of **PTZ1**, increasing from **PTZ2** to **PTZ5** and **PTZ6**, once again in agreement with the presence of the electronrich thiophene spacer.

Dye-sensitized solar cells

Though it was not the main scope of this work, **PTZ1-6** were first tested in DSSCs in order to have a broader evaluation of the new dyes as photosensitizers. DSSCs have been prepared using a single layer film (10 μm) consisting of a blend of active 20-nm up to 450-nm scattering nanoparticles of TiO_2 anatase and Z960 [54] (1.0 M dimethyl imidazolium iodide, 0.03 M I_2, 0.05 M LiI, 0.1 M guanidinium thiocyanate and 0.5 M 4-*t*-butylpyridine in acetonitrile/valeronitrile 85/15) as the liquid electrolyte. Chenodeoxycholic acid (CDCA) was added as a de-aggregating co-adsorbent agent (CDCA:dye = 1:1).[55] Current (*J*)/voltage (*V*) curves and incident photon-to-current conversion efficiencies (IPCE) are shown in Fig. 6. With the exception of **PTZ6**, for which low current and voltage values were recorded, photocurrent values and corresponding PCE of the devices sensitized by the thiophene-based dyes were larger than **PTZ1**-based DSSC, in agreement with the enhanced optical properties.

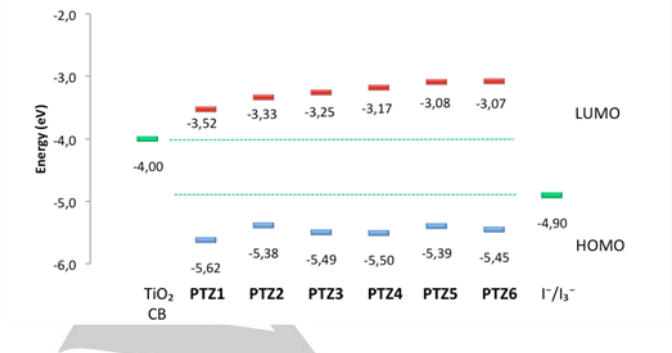

Fig. 5: HOMO/LUMO energies of dyes **PTZ1-PTZ6** in comparison with the conduction band (CB) level of TiO_2 and redox potential of the couple I^-/I_3^-.

Devices based on dyes **PTZ1-6** exhibited different photovoltages, spanning from 604 to 682 mV. Dye **PTZ5** yielded the highest photovoltage, which in turn determined the largest PCE (> 6%) in the series. Electrochemical impedance spectroscopy (EIS) was used to further investigate the comparative behaviour, in particular in terms of different photovoltages, of the DSSC based on the dyes **PTZ1-6**.[52,56] The analysis of the impedance spectra was performed in terms of Nyquist plots (see Fig. S2) where the imaginary part of the impedance is plotted as a function of the real part over the range of frequencies. The impedance of the cell can be described by an equivalent circuit model (see inset Fig. S2) in which the different cell components and their interfaces are treated as discrete electrical elements. Under illumination at open circuit voltage conditions, in order to have direct current equal to zero and force the device to mainly describe recombination phenomena, the properties of the TiO_2/electrolyte interface can be derived from the main (central) arc in terms of recombination resistance (R_{rec}), related to the recombination current, and chemical capacitance, associated to the density of states in the band gap of the oxide (C_μ). The apparent electron lifetime in the oxide τ_n can thus be calculated from $\tau_n = R_{rec} \times C_\mu$ and corresponds to the angular frequency at the top of the middle arc of the Nyquist plots.[52] All of these parameters are therefore associated to charge transfer (recombination) phenomena representing detrimental back-processes between the injected electrons in the semiconductor oxide and the oxidized form of the electrolyte. According to the benchmark Shockley–Queisser model the most important limitations to the cell photovoltage are carrier recombination phenomena, which are thus summarized in the τ_n values, included in Table 3 (see Table S1 for R_{rec} and C_μ values†). Indeed, we observe that the τ_n values were closely associated to the measured photovoltages. Accordingly, the cell based on **PTZ5**, which exhibited the highest carrier lifetime, showed the largest voltage, whereas the lowest voltages observed for DSSC sensitized by **PTZ3**, **PTZ4**, and **PTZ6** were associated to the smallest lifetimes. The analysis of the two components R_{rec} and C_μ showed that the highest electron lifetime measured for **PTZ5** was mainly due to the contribution of the chemical capacitance. Looking at the peculiar structural features of **PTZ5** we might therefore conclude that the most favourable conditions for the device photovoltage are associated to the presence of the alkyl groups on the thiophene rings, beneficial in terms of suppressing recombination reactions as widely reported in the literature,[26,57–59] with particular emphasis on the position of the substituents in the dye central moiety.[27,54,60,61] We note that these beneficial effects for **PTZ5** are nicely confirmed by the experimental findings in the photocatalytic hydrogen production (*vide infra*).

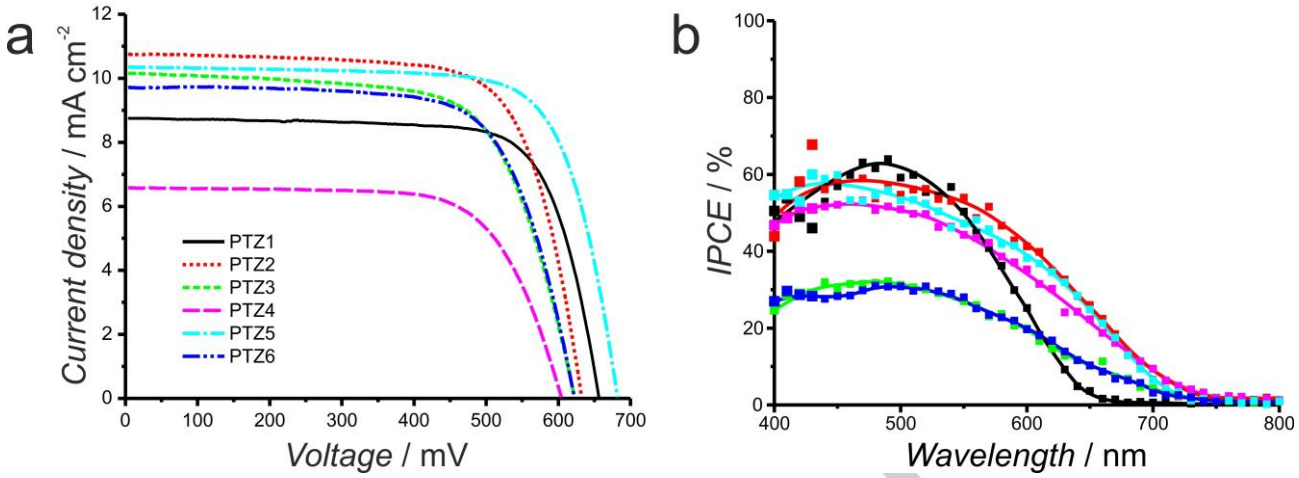

Fig. 6. a) *J*/*V* characteristics of **PTZ1-6** sensitized solar cells under full AM 1.5 solar intensity; b) IPCE plots: the TiO_2 film thickness is a 10-µm opaque active layer.

Table 3: Photovoltaic characteristics of DSSCs containing phenothiazine-based dyes **PTZ1-6** (AM1.5 solar light).[a]

Dye[b]	J_{sc} [mA cm^{-2}]		V_{oc} [mV]		FF [%]		PCE [%]		τ_e [ms][c]
PTZ1	8.76	(11.1)	656	(667)	74	(74)	4.3	(5.5)	3.1
PTZ2	10.8	(13.4)	632	(649)	72	(70)	4.9	(6.1)	2.6
PTZ3	10.2	(13.1)	622	(632)	67	(66)	4.3	(5.5)	1.8
PTZ4	9.71	(12.7)	622	(632)	70	(67)	4.2	(5.3)	2.2
PTZ5	10.3	(12.0)	682	(690)	74	(74)	5.2	(6.1)	5.0
PTZ6	6.58	(9.00)	604	(614)	69	(68)	2.8	(3.7)	1.7
N719[d]	14.7	(17.4)	768	(753)	73	(71)	8.3	(9.3)	

[a] Values without a black mask on the top of the cell are listed in brackets. [b] Dye solution of 2 x 10^{-4} M in EtOH with 1:1 CDCA; electrolyte Z960 (see text), single TiO_2 layer (10 µm); surface area 0.20 cm^2. [c] Apparent electron lifetime. [d] Dye solution of 5 x 10^{-4} M in EtOH solution with 1:1 CDCA; electrolyte A6141 (0.6 M *N*-butyl-*N*-methyl imidazolium iodide, 0.03 M I_2, 0.10 M guanidinium thiocyanate, and 0.5 M 4-*t*-butylpyridine in acetonitrile/valeronitrile 85:15).

Hydrogen production using dye-sensitized Pt/TiO_2

Hydrogen production using Pt/TiO_2 sensitized by dyes **PTZ1–6** was investigated using a Pt/TiO_2 nanocomposite catalyst prepared by irradiation of Degussa P25 TiO_2 suspended in a water/EtOH solution containing $Pt(NO_3)_2$. Irradiation with a UV-Vis lamp results in the reduction of Pt^{2+} ions and deposition of Pt(0) nanoparticles on the surface of the TiO_2 support. The powder X-ray diffraction (PXRD) analysis revealed that the material contains ~ 68% of anatase and ~ 32% of rutile (see Rietveld refinement in Fig. S3). The broadening of the main reflections of anatase and rutile phases indicates a mean crystallite size of 20 and 19 nm, respectively. No reflections related with Pt nanoparticles were observed in the PXRD pattern of the Pt/TiO_2 material because of their low amount and nanometric size.

Textural analysis by means of N_2 physisorption revealed that the material shows a type IV isotherm, typical of mesoporous materials (see Fig. S4a).[62] The specific surface area, calculated applying the Brunauer-Emmett-Teller (BET) equation, is 54 m^2 g^{-1} while the Barrett-Joyner-Halenda (BJH) analysis showed that the pores of the materials have a maximum around 50 nm and a cumulative volume of 0.232 mL g^{-1} (Fig. S4b).

Representative transmission electron microscopy (TEM) images acquired on the Pt/TiO_2 material are presented in Fig. 7a-b. TiO_2 particles show an irregular shape, with dimensions of 10-40 nm, in good agreement with the crystallite sizes calculated from line broadening in PXRD analysis. Pt nanoparticles, as highlighted in high-angle annular dark-field scanning TEM (HAADF-STEM) images (Fig. 7c), were homogeneously distributed on the surface of TiO_2 particles. Their size distribution (Fig. 7d) showed a mean particle size of 2.4 nm, in agreement with the size of metal nanoparticles obtained by photodeposition on multiphasic TiO_2 supports.[11,14,63–66]

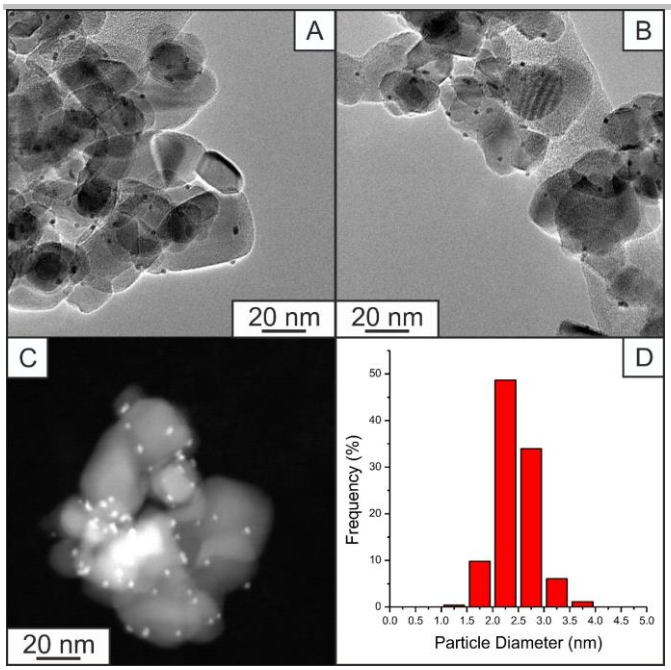

Fig. 7: a,b) Representative transmission electron microscopy (TEM) images acquired on the Pt/TiO_2 material; c) HAADF-STEM image showing distribution of Pt nanoparticles on the surface of TiO_2 support; d) Size distribution of the Pt nanoparticles.

The **PTZ1**–**6** dyes were used as sensitizers in the Pt/TiO_2 material for H_2 production under visible irradiation using triethanolamine (TEOA) as sacrificial agent at pH = 7.0. The **PTZ1-6** were quantitatively adsorbed on the Pt/TiO_2 catalyst from their solution in EtOH. After adsorption, the remaining solution was colourless. Under irradiation with visible light (λ > 420 nm), the H_2 production rates obtained using Pt/TiO_2 sensitized by **PTZ1-6** dyes are presented in Fig. 8 while the overall H_2 productivities are presented in Fig. S5. After optimization of the experimental conditions following the indications reported by Kisch and Bahnenmann,[67] the H_2 production rates are reported in Fig 8 and in Fig. S5 after normalization to the mass of the catalyst. This is intended to give an indication of the scalability of the process under comparable experimental conditions. Notably, unlike previous reports on phenothiazine-functionalized Pt/TiO_2,[28] in this study we extended the irradiation time up to 20 h in order to study the stability of the present photocatalysts under reaction conditions.

The data reported in Fig. S5 evidenced that the overall H_2 productivity of the photocatalysts functionalized with the new thiophene-based phenothiazine **PTZ2-6** were lower than that obtained using the reference dye **PTZ1** reported by Lee et al.,[28] though the dibutoxy-thiophene derivative **PTZ5** showed an H_2 productivity comparable to that of the **PTZ1**-based photocatalyst. The remaining dyes **PTZ2-4** and **PTZ6** showed a comparable activity. Despite the overall hydrogen production of the new dyes was lower than that of the reference system, the analysis of the H_2 production rates, presented in Fig. 8, put in evidence highly

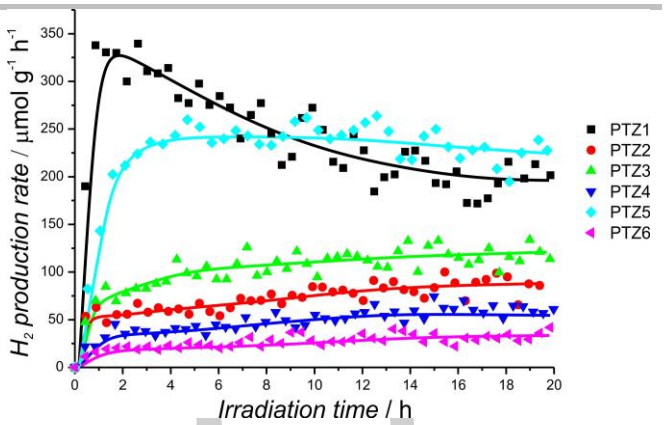

Fig. 8: H_2 production rates measured using the dye/Pt/TiO_2 materials in H_2 production from TEOA 10 v/v% solution at pH = 7.0 under irradiation with visible light (λ > 420 nm).

Table 4: Photocatalytic performance of the dye/Pt/TiO_2 materials in H_2 production from TEOA 10 v/v% solution at pH = 7.0 under irradiation with visible light (λ > 420 nm).

Sample	Dye loading (µmol/50mg)	H_2 amount [a] (µmol)	TON [b]	LFE_{03} [c]	LFE_{20} [d]
PTZ1	2.97	121.7	81.8	0.144%	0.090%
PTZ2	2.98	35.8	24.0	0.026%	0.039%
PTZ3	3.01	52.1	34.6	0.037%	0.048%
PTZ4	2.99	24.9	16.6	0.017%	0.027%
PTZ5	2.98	111.6	74.9	0.104%	0.103%
PTZ6	2.98	13.6	9.1	0.010%	0.014%

[a] Overall H_2 amount produced after 20 h of irradiation; [b] TON = (2 x H_2 amount) / (dye loading); [c] Light-to-Fuel Efficiency calculated after 3 h of irradiation; [d] Light-to-Fuel Efficiency calculated after 20 h of irradiation.

significant insights. Indeed, the **PTZ1**-based photocatalysts showed a maximum in the H_2 production rate after 2 hours of irradiation, followed by a progressive decrease of its activity, in agreement with reports in the literature (Fig. S6).[28,29] On the contrary, the photocatalysts functionalized with the new **PTZ2-6** dyes showed an initial activation period of 4 – 6 h, resulting in an even low but constant H_2 production rates up to 20 h of irradiation under visible light, a behavior which is unprecedented in the literature for this type of sensitizers. Notably, the H_2 production rate of the **PTZ5**-based photocatalyst surpassed that of the **PTZ1**-based one after 8 h of irradiation. The straightforward stability demonstrated by the photocatalysts functionalized with the new thiophene-based phenothiazines is particularly important in view of a medium-long term utilization of dye-sensitized photocatalysts for H_2 production.

Table 4 summarizes the photocatalytic performance of the dye-sensitized material studied in this work. Turn-Over Numbers (TON), calculated accordingly to the procedure previously reported in the literature,[28,29] indicate how many electrons generated by excitation of the dye are effective for proton reduction and H_2 production. The obtained data confirmed that the efficiency of the photocatalyst sensitized with **PTZ5**

approaches that of the benchmark **PTZ1**, with all the other dyes showing lower TON values. This fact could be associated with the presence of thiophene spacers that could strongly interact with the surface of Pt nanoparticles, covering the catalytic sites responsible for H_2 evolution. In the case of **PTZ5**, adsorption of the sulphur sites on the Pt nanoparticles could be in some way hindered by the alkyl chains on the thiophene spacer. Moreover, degradation of the **PTZ1-6** dyes could contribute to the trend observed in the TON values (see below). The TON obtained in this study are significantly lower with respect to those reported in the literature for photocatalysts sensitized using dyes with similar molecular structure.[28,29] However, we note that the photocatalytic H_2 production is strongly dependent on many experimental conditions, including irradiation power, reactor geometry and dye loading on the photocatalysts.[67] Therefore, the direct comparison of TON values is meaningful only when the same experimental conditions and apparatus are used.

Light-to-Fuel Efficiency (LFE) has been introduced in order to quantitatively evaluate the fraction of energy from the light source that is stored in the form of H_2, defined in a similar manner as that previously proposed for H_2 production using photoelectrochemical cells [68] or photocatalytic reforming of oxygenated compounds.[69] LFE listed in Table 4 have been calculated from the H_2 flow produced at different irradiation times: 3 h (LFE_{03}) and 20 h (LFE_{20}). The LFE values confirmed the superior efficiency of **PTZ1** and **PTZ5** in storing light energy into chemical energy compared to the other dyes. Notably, LFE decreases with time for **PTZ1** while it is almost constant for the thiophene-derived dyes **PTZ2-6**. As a result, the LFE_{20} is significantly higher for the thiophene-substituted dye **PTZ5** compared to the reference benchmark **PTZ1**.

Dye degradation study and intrinsic photocatalytic activity

As aforementioned, we investigated the dye-sensitized production of hydrogen over irradiation times up to 20 h, in contrast with the much shorter irradiation periods commonly used in the literature, which, apart rare exceptions,[29] are typically around 5 h. The selected experimental time is a compromise between the need of performing longer stability tests and that of avoiding appreciable changes in the concentration of the sacrificial agent due to conversion of sacrificial agent, accumulation of by-products, and selective evaporation of the solvent in the used flow reactor. In particular, we were attracted by the anomalous behavior of the reference dye **PTZ1** after the first irradiation hours, both in our investigation (Fig. 8) and in the literature reports (Fig. S6).[28,29] In order to get deeper insights into such experimental findings and previous literature studies, we decided to perform a detailed investigation of the stability of the **PTZ1-6** dye-sensitized Pt/TiO_2 catalysts over 20 h under the same conditions used during the hydrogen measurements (Fig. 8). The stability has been

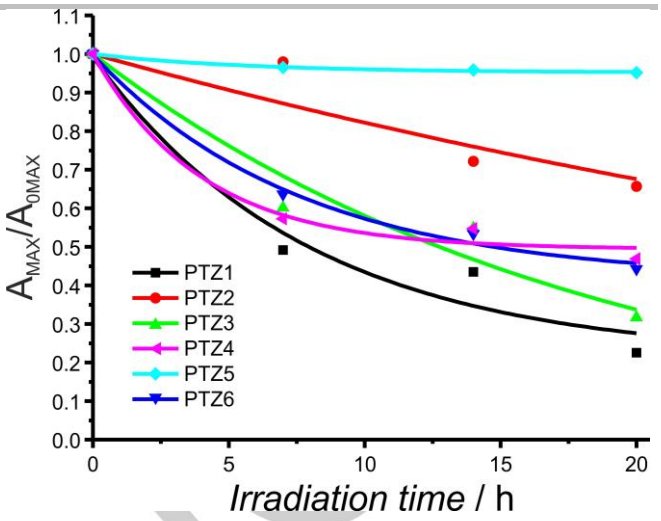

Fig. 9: Degradation plots of the **PTZ1-6** dye-sensitized Pt/TiO_2 catalysts under visible irradiation using TEOA as a sacrificial agent at pH = 7.0 in water under a nitrogen atmosphere.

ascertained via optical absorption of a proper solution of the desorbed dyes from the Pt/TiO_2 catalyst at specific irradiation times and reported as relative residual absorbance compared to the absorbance before irradiation (t = 0 h). The results are summarized in Fig. 9.

The degradation study clearly shows that all of the dyes, with the notable exception of the catalyst sensitized by dye **PTZ5**, for which the best hydrogen production rates were recorded over longer irradiation times, are not stable under visible irradiation. Very importantly, the largest degradation over 20 h was observed for the reference literature dye **PTZ1**, for which the residual active catalyst after 20 h of irradiation is ~ 30%. In other terms, the catalyst based on the literature dye **PTZ1** is mostly decomposed after 20 h. This finding clearly explains the irregular behavior recorded both in our investigation (Fig. 8) and in the literature (Fig. S6),[28,29] and visibly stresses the insufficient reliability of photocatalytic studies over short irradiation times (4-5 h). Apart the catalyst sensitized by **PTZ5**, those sensitized by the new dyes experiences photo-degradation as well, although the extent was smaller, with residual active catalyst being between ~35 and 70% after 20 h. While the reason of the superior stability of the dyes **PTZ2-6** compared to the dye **PTZ1** is not straightforward, it is evident that the presence of the thiophene spacer resulted beneficial for improved stability under light. This can be correlated both to the stronger interaction between the dyes and the Pt/TiO_2 catalyst mediated by the presence of the sulphur atoms of the thiophene-base spacer, somewhat inhibiting the degradation catalytic activity of the photocatalyst, and to the improved stability of the dye radical cation $D^{\cdot+}$ following the electron photoinjection.[70]

Very remarkably, the catalyst based on **PTZ5** is the only one stable over the whole irradiation period, thus elegantly validating the recorded superior performance of the hydrogen production over longer irradiation times (Fig. 9). The improved stability

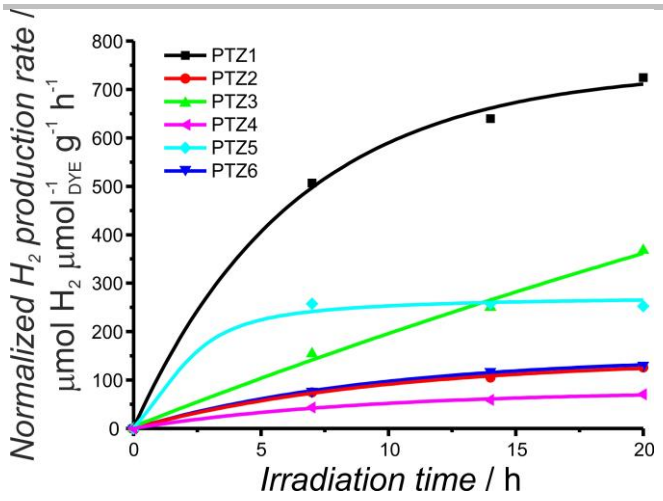

Fig. 10: Actual H_2 production rates (measurement conditions described for Fig. 7) normalized by the fraction of residual non-decomposed catalyst.

might be associated to the presence of the alkyl chains on the spacer groups of **PTZ5**, being this the main peculiar structural difference with respect to the other thiophene derivatives. This conclusion is in full agreement with the EIS investigation on DSSC (*vide infra*) suggesting that interface interactions (e.g. dye regeneration or charge recombination) or intermolecular interactions (intermolecular self-quenching) may play a role in determining the stability in hydrogen production experiments. It is not evident if the stability of **PTZ5** is due to the peculiar D-π-A structure as a whole or rather to the presence of an inherently more stable spacer. The bis-alkoxythiophene groups do not induce a larger stability by itself, since, for instance, polycyclic thiophene cores, such as the thienothiophene groups in **PTZ3**, are more stable thanks to their larger structural rigidity.[71–74] We thus conclude that is the embedding of the bis-alkoxythiophene spacers in the phenothiazine donor-acceptor structure which accounts for the higher stability, with a key role of the four alkyl substituents strategically located in the middle portion of the molecular assembly, as previously discussed. Conversely, we exclude relevant electronic effects associated to the presence of the donor alkoxy groups on the thiophene ring, since these groups are present also in the EDOT derivative **PTZ6** where no improved stability was observed.

The photocatalytic production of hydrogen rates were also calculated by normalizing the data of Fig. 8 to the residual, non-decomposed dyes (meaning the hydrogen production per effective dye quantity left in the device after photodegradation), as measured at the different irradiation times. The results are depicted in Fig. 10.

The data of Fig. 10 clearly indicated relevant aspects. First, and likely more importantly, the profile of the production rate of the reference catalyst sensitized by **PTZ1** is now regular throughout the whole 20 h irradiation period. Therefore, the hydrogen production rates per gram of catalyst reported in the literature (Fig. S6) and confirmed in our study (Fig. 8) offers only a partial view of a complex process and they do not take into account the intrinsic properties of the dye-sensitized catalyst, potentially leading to misleading conclusions in terms of property/structure relationships. Second, the new dyes are less efficient than the reference dye **PTZ1**, when net production rates are taken into account (Fig. 10). This lower performance are reasonably associated to the strong and preferential interaction that sulphur atoms of the thiophene-base spacers can establish with surface platinum atoms, inhibiting the catalytic activity of Pt by poisoning. The specific lower activity is well compensated by the improved stability of the dyes opening perspectives for real long-term applications by the design of new catalysts based on sulphur-free organic dyes. Third, the measured TON, LFE_{03}, and LFE_{20} can be correlated to dye stability. The TON of a catalyst describes how many cycles it is able to cycle through before becoming inactive. It is therefore evident that the dye degradation plays a key role in defining the catalyst TON. In particular, in the thiophene-based series, the highest measured TON and LFE (**PTZ5**) are associated to the most stable dye. Finally, and most importantly in terms of structure/property relations, the intrinsic hydrogen production of the catalysts based on **PTZ2-6** can now be, at least in some cases, correlated to the optical properties of the dyes, though reminding that the light harvesting efficiency is only one of the components controlling the photocatalytic activity. Therefore the new picture changes the unprocessed experimental hydrogen production trend depicted in Fig. 8, in which no apparent correlation between hydrogen evolution and optical properties is present. More specifically, the catalyst based on **PTZ3**, that is the dye with the highest molar absorptivity in the thiophene-based series (Table 1), is now found as the most efficient system. Following the same analysis, the catalyst based on **PTZ2**, that is the dye with the lowest molar absorptivity in the thiophene-based series, is found to be one of the least effective systems.

Conclusions

We have designed and investigated a series of phenothiazine-based donor-acceptor dyes for dye-sensitized photocatalytic hydrogen production from water and dye-sensitized solar cells. The series is characterized by having different thiophene-based π-spacers, from the simple thiophene ring to the alkoxy-substituted thiophene derivatives. The introduction of the thiophene-based π-spacers afforded significantly enhanced optical properties both in terms of longer wavelength absorption and molar absorptivities, with up to a four-fold increase compared to the reference dye **PTZ1**.

Pt/TiO_2 photocatalysts sensitized by dyes **PTZ1-6** showed a remarkable H_2 productivity from TEOA aqueous solution at pH = 7.0 under irradiation with visible light for long irradiation times (20 h). The preferred longer irradiation times are in contrast with previously reported experimental conditions, which typically use much shorter irradiation periods (2-5 h). Although the photocatalyst sensitized by the dye **PTZ1** without the thiophene spacers demonstrated the highest initial H_2 production rate, it undergoes a progressive deactivation with irradiation time, a behavior commonly reported, but so far not clearly rationalized, for this class of dyes. Such characteristic is critical for practical long-term applications. On the contrary, photocatalysts sensitized with the new substituted **PTZ2-6** dyes revealed improved stability after longer irradiation times and enhanced performances after an initial activation period.

An unprecedented degradation study has revealed for the first time that the anomalous photocatalytic activity of the catalyst sensitized by the reference dye **PTZ1** is the clear consequence of the strong degradation of the dye with irradiation times. The overall picture of the intrinsic

photocatalytic activity (Fig. 10), that is the hydrogen production per effective dye quantity left in the device after photodegradation, is significantly altered compared to the direct experimental data (Fig. 8), thus revealing the true dye-sensitized catalyst activity and allowing accurate structure/property relations, helpful for future design. In particular, we have found that the intrinsic photocatalytic activity is related to the optical properties, at variance with unprocessed experimental data, thus validating our design.

Notably, the new dye **PTZ5** is a promising candidate for efficient dye-sensitized photocatalytic H_2 production, with stable H_2 production rate and an overall productivity comparable to that of the reference compound **PTZ1**. The degradation investigation has evidenced that this finding is the direct consequence of the remarkable stability of **PTZ5** under irradiation, though the intrinsic photocatalytic efficiency was lower than that of the reference dye.

Experimental Section

General information

NMR spectra were recorded with a Bruker AMX-500 spectrometer operating at 500.13 MHz (^{1}H) and 125.77 MHz (^{13}C). Coupling constants are given in Hz. Absorption spectra were recorded with a V-570 Jasco spectrophotometer. Infrared spectra (IR) were recorded with an ATR-FTIR Perkin–Elmer Spectrum100 spectrometer. Flash chromatography was performed with Merck grade 9385 silica gel 230–400 mesh (60 Å). Reactions performed under inert atmosphere were done in oven-dried glassware and a nitrogen atmosphere was generated with Schlenk technique. Conversion was monitored by thin-layer chromatography by using UV light (254 and 365 nm) as a visualizing agent. All reagents were obtained from commercial suppliers at the highest purity grade and used without further purification. Anhydrous solvents were purchased from Sigma-Aldrich and used without further purification. Extracts were dried with Na_2SO_4 and filtered before removal of the solvent by evaporation.

FTO-coated glass plates (2.2 mm thick; sheet resistance ~7 ohm per square; Solaronix), Dyesol 18NR-AO active opaque TiO_2 blend of active 20 nm anatase particles and up to 450 nm anatase scatter particles, and N719 (Sigma-Aldrich) have been purchased from commercial suppliers. UV-O_3 treatment was performed using Novascan PSD Pro Series – Digital UV Ozone System. The thickness of the layers was measured by means of a VEECO Dektak 8 Stylus Profiler.

Electrochemical characterization

Pulsed Voltammetry (DPV) and Cyclic Voltammetry (CV) were carried out at scan rate of 20 and 50 mV/s, respectively, using a PARSTA2273 potentiostat in a two compartments, three electrode electrochemical cell in a glove box filled with N_2 ([O_2] and [H_2O] ≤ 0.1 ppm). The working, counter, and the pseudo-reference electrodes were a glassy carbon pin, a Pt flag and an Ag/AgCl wire, respectively. The working electrodes discs were well polished with alumina 0.1 µm suspension, sonicated for 15 min in deionized water, washed with 2-propanol, and cycled for 50 times in 0.5 M H_2SO_4 before use. The Ag/AgCl pseudo-reference electrode was calibrated, by adding ferrocene (10^{-3} M) to the test solution after each measurement.

Oxidation potential values were determined using DPV traces by following the reference methods reported in the literature.[75] For mono-electronic well defined current wave, the potentials were calculated by the peak position. In the presence of overlapping peaks due to molecular additional oxidations, potential values were calculated using the current onsets of the oxidation processes for both the standard (ferrocene) and the molecules.

Fabrication of the DSSCs

DSSCs have been prepared adapting a procedure reported in literature.[76] In order to exclude metal contamination all of the containers were in glass or Teflon and were treated with EtOH and 10% HCl prior to use. Plastic spatulas and tweezers have been used throughout the procedure. FTO glass plates were cleaned in a detergent solution for 15 min using an ultrasonic bath, rinsed with pure water and EtOH. After treatment in a UV-O_3 system for 18 min, the FTO plates were treated with a freshly prepared 40 mM aqueous solution of $TiCl_4$ for 30 min at 70 °C and then rinsed with water and EtOH. An opaque active layer of 0.20 cm^2 was screen-printed using Dyesol 18NR-AO active opaque TiO_2 paste. The coated films were thermally treated at 125 °C for 6 min, 325 °C for 10 min, 450 °C for 15 min, and 500 °C for 15 min. The heating ramp rate was 5 - 10 °C/min. The sintered layer was treated again with 40 mM aqueous $TiCl_4$ (70 °C for 30 min), rinsed with EtOH and heated at 500 °C for 30 min. After cooling down to 80 °C the TiO_2 coated plates were immersed into a solution of the dye for 20 h at room temperature in the dark.

Counter electrodes were prepared according to the following procedure: a 1-mm hole was made in a FTO plate, using diamond drill bits. The electrodes were then cleaned with a detergent solution for 15 min using an ultrasonic bath, 10% HCl, and finally acetone for 15 min using an ultrasonic bath. After thermal treatment at 500 °C for 30 min, 15 µL of a 5 mM solution of H_2PtCl_6 in EtOH was added and the thermal treatment at 500 °C for 30 min repeated. The dye adsorbed TiO_2 electrode and Pt-counter electrode were assembled into a sealed sandwich-type cell by heating with a hot-melt ionomer-class resin (Surlyn 30-µm thickness) as a spacer between the electrodes. A drop of the electrolyte solution was added to the hole and introduced inside the cell by vacuum backfilling. Finally, the hole was sealed with a sheet of Surlyn and a cover glass. A reflective foil at the back side of the counter electrode was taped to reflect unabsorbed light back to the photoanode.

Photovoltaic and photoelectrical characterization of DSSCs

Photovoltaic measurements of DSSCs were carried out with an antireflective layer and with or without black mask on top of the photoanode of 0.38 cm^2 surface area under a 500 W Xenon light source (ABET Technologies Sun 2000 class ABA Solar Simulator). The power of the simulated light was calibrated to AM 1.5 (100 mW cm^{-2}) using a reference Si cell photodiode equipped with an IR-cutoff filter (KG-5, Schott) to reduce the mismatch in the region of 350-750 nm between the simulated light and the AM 1.5 spectrum. Values were recorded after 3 and 24 h, 3 and 6 days of ageing in the dark. I–V curves were

obtained by applying an external bias to the cell and measuring the generated photocurrent with a Keithley model 2400 digital source meter. Incident photon-to-current conversion efficiencies (IPCE) were recorded as a function of excitation wavelength by using a monochromator (Omni 300 LOT ORIEL) with single grating in Czerny-Turner optical design, in AC mode with a chopping frequency of 1 Hz and a bias of blue light (0.3 sun).

EIS spectra were obtained using an Eg&G PARSTAT 2263 galvanostat potentiostat. The analysis of the impedance spectra has been performed in terms of Nyquist plots. In this experiment a small sinusoidal voltage stimulus of a fixed frequency is applied to an electrochemical cell and its current response measured. The measurements have been performed in the frequency range from 100 kHz to 100 mHz under ac stimulus with 10 mV of amplitude and no applied voltage bias. The obtained Nyquist plots have been fitted via a non-linear least square procedure using the equivalent circuit model in Fig. S2.

Preparation of Pt/TiO_2 nanopowders

Platinization of TiO_2 Degussa P25 was done through a photodeposition method known in literature.[Error! Bookmark not defined.a,Error! Bookmark not defined.a,Error! Bookmark not defined.] TiO_2 Degussa P25 (2.0 g) was suspended in a solution of H_2O (200 mL) and EtOH (200 mL) containing 32.7 mg of $Pt(NO_3)_2$, in order to reach a final metal loading of 1.0 wt%. After stirring for 1 h in the dark, the suspension was irradiated with a 450 W medium pressure lamp for 4 h. Nanopowders were recovered through centrifugation, washed with EtOH 3 times, and dried under vacuum at 50 °C overnight.

Characterization of Pt/TiO_2 nanopowders

Phase composition has been analyzed by Powder X-ray Diffraction (PXRD) using a Philips X'Pert diffractometer using a Cu Kα (λ = 0.154 nm) X-ray source in the range $10° < 2\theta < 100°$ and data were analyzed by using the PowderCell 2.0 software. Mean crystallite sizes were calculated applying the Scherrer's equation to the principal reflection of each phase [(101) for anatase and (110) for rutile].

Textural properties of the catalyst have been analyzed by N_2 physisorption at the liquid nitrogen temperature using a Micromeritics ASAP 2020 automatic analyzer. The samples were previously degassed under vacuum at 200°C overnight. Specific surface area has been determined applying the BET method to the adsorption isotherm in the range $0.10 < p/p^0 < 0.35$. Pore size distribution has been evaluated applying the BJH theory to the desorption branch of the isotherm.**Error! Bookmark not defined.**

The morphology of the composite materials and the distribution of the supported Pt nanoparticles were evaluated by High Resolution Transmission Electron Microscopy (HR-TEM) and High Angle Annular Dark Field-Scanning Transmission Electron Microscopy (HAADF-STEM) images recorded by a JEOL 2010-FEG microscope operating at the acceleration voltage of 200 kV. The microscope has 0.19 nm spatial resolution at Scherzer defocus conditions in HR-TEM mode and a probe of 0.5 nm was used in HAADF-STEM mode.

Adsorption of PTZ1-6 dyes on Pt/TiO_2

Dye staining was done by suspending 200 mg of Pt/TiO_2 nanopowders in 20 mL of dye solution (0.3 mM in ethanol) for 24 h in the dark. Then nanopowders were separated through centrifugation, washed twice with ethanol, and dried under vacuum at room temperature overnight. After adsorption, the concentration of the dyes in the solution was measured by UV-Vis spectroscopy, confirming that the loading of dyes on the Pt/TiO_2 material is quantitative.

Hydrogen production through water splitting

The **PTZ1-6**-functionalized Pt/TiO_2 nanomaterials have been tested for H_2 production adapting the procedure reported by Lee et al.**Error! Bookmark not defined.** Photocatalytic experiments were performed in an apparatus described in a previous paper.**Error! Bookmark not defined.**[a] 50 mg of the **PTZ1-6**-functionalized Pt/TiO_2 catalyst was suspended into 60 mL of 10% v/v aqueous solution of triethanolamine (TEOA) previously neutralized with HCl. After purging with Ar (15 mL min^{-1}) for 30 min, the suspension was irradiated using a 150 W Xe lamp with a cut-off filter at 420 nm. Irradiance was ~ 6 x 10^{-3} W m^{-2} in the UV-A range and ~ 1080 W m^{-2} in the visible range (400 – 1000 nm). The concentration of H_2 in gas stream coming from the reactor has been quantified using a Agilent 7890 gaschromatograph equipped with a TCD detector, connected to a Carboxen 1010 column (Supelco, 30 m x 0.53 mm ID, 30 µm film) using Ar as carrier. Notably, the amount of catalyst has been optimized following the indications recently presented by Kisch and Bahnenmann[Error! Bookmark not defined.]. The optimization has been performed using the **PTZ5**-sensitized catalyst, increasing the amount of catalyst employed until the optimal H_2 production rate has been obtained (further addition of catalyst did not afford increased production of H_2).

The performances of the **PTZ1-6** sensitized photocatalysts have been reported in terms of H_2 production rate and overall H_2 productivity. Turn-Over Numbers (TON) were calculated as (2 x overall H_2 amount) / (dye loading). Light-to-Fuel Efficiency (LFE) was calculated as:

$$LFE = \frac{F_{H_2} * \Delta H^0_{H_2}}{S * A_{irr}}$$

where F_{H_2} is the flow of H_2 produced (expressed in mol s^{-1}), $\Delta H^0_{H_2}$ is the enthalpy associated with H_2 combustion (285.8 kJ mol^{-1}), S is the total incident light irradiance, as measured by adequate radiometers in 400 – 1000 nm ranges (expressed in W cm^{-2}) and A_{irr} is the irradiated area (expressed in cm^2).

Degradation measurements of dye-sensitized Pt/TiO_2

The degradation of the dye-sensitized catalysts has been investigated by means of optical absorption of the desorbed dye after specific irradiation times. The UV-Vis spectrum of a known amount of dye-sensitized Pt/TiO_2 catalyst, prepared as described above, has been measured for each sample by completely desorbing the dye using a known volume of a 0.1 M solution of NaOH in ethanol–H_2O (1:1). The resulting suspension has been filtered using a 0.45 µm PTFE syringe filter and the UV-Vis spectrum measured in the spectral range 320–800 nm, using a quartz cuvette with a 1-cm optical path. Spectra were collected at different irradiation times (7, 14, and 20 h) under the

same experimental conditions of the hydrogen production measurements. The spectra collected before irradiation (t = 0 h) were used as reference data. Degradation data have been reported as relative residual absorbances A_{max}/A_{0max}, where A_{max} and A_{0max} are the absorbances of the desorbed dyes recorded at their Vis absorption peaks after and before irradiation, respectively.

Synthetic procedures

General Procedure A for Suzuki-Miyaura Cross-Coupling: Product **1** (1 eq.) and Pd(dppf)Cl_2·CH_2Cl_2 (10 % eq.) were dissolved in dimethoxyethane (0.1 M) and stirred for 15 minutes under nitrogen atmosphere. Then boronic acid/ester derivative (2.4 eq.) and K_2CO_3 (10 eq.) were added as suspension in methanol (0.1 M). The reaction was performed with microwave irradiation (100 °C, 200 W, 90 minutes) and then quenched by pouring into a saturated solution of NH_4Cl (50 mL). Filtration on Celite and extractions with organic solvent allowed to isolate the crude product, then purified through column chromatography on silica gel.

General Procedure B for Suzuki-Miyaura Cross-Coupling: Bromo-derivative (2.2 eq.) and Pd(dppf)Cl_2·CH_2Cl_2 (10 % eq.) were dissolved in dimethoxyethane (0.1 M) and stirred for 15 minutes under nitrogen atmosphere. Then product **4** (1 eq. of crude product) and K_2CO_3 (10 eq.) were added as suspension in methanol (0.1 M). The reaction was performed with microwave irradiation (100 °C, 200 W, 90 minutes) and then quenched by pouring into a saturated solution of NH_4Cl (50 mL). Filtration on Celite and extractions with organic solvent allowed to isolate the crude product, then purified through column chromatography on silica gel.

General Procedure C for Knoevenagel Condensation: Aldehyde precursor (1 eq.), cyanoacetic acid (10 eq.) and piperidine (10 eq. + catalytic) were dissolved in $CHCl_3$ (0.02 M) and warmed to reflux for 5 h. After having the solvent evaporated, a solution of HCl 1 M (~50 mL) was added and the mixture was left under magnetic stirring for 5 h at rt. The dark red solid that precipitated was filtered and washed with water (3x30 mL), PE (2x30 mL) and Et_2O (1x10 mL).

5,5'-(10-octyl-10*H*-phenothiazine-3,7-diyl)dithiophene-2-carbaldehyde (2). Product **2** was synthetized according to general procedure A for Suzuki-Miyaura cross-coupling, using product **1** (200 mg, 0.43 mmol), Pd(dppf)Cl_2·CH_2Cl_2 (35 mg, 0.043 mmol), (5-formylthiophen-2-yl)boronic acid (160 mg, 1.03 mmol), K_2CO_3 (600 mg, 4.3 mmol), DME (3 mL) and methanol (3 mL). Extractions were performed with AcOEt (3 x 50 mL) and a mixture of PE:AcOEt - 3:1 was used as eluent for purification. The desired product was isolated as a red solid (200 mg) with a 87% of yield. ^{1}H NMR (500 MHz, $CDCl_3$): δ 9.82 (s, 2H), 7.65 (d, *J* = 3.9 Hz, 2H), 7.38 (dd, *J* = 8.5, 2.0 Hz, 2H), 7.31 (d, *J* = 2.0 Hz, 2H), 7.24 (d, *J* = 3.9 Hz, 2H), 6.79 (d, *J* = 8.5 Hz, 2H), 3.79 (t, *J* = 7.2 Hz, 2H), 1.81 – 1.71 (m, 2H), 1.44 – 1.34 (m, 2H), 1.34 – 1.18 (m, 8H), 0.84 (t, *J* = 6.9 Hz, 3H). ^{13}C NMR (126 MHz, $CDCl_3$): δ 182.5, 153.1, 145.1, 141.7, 137.6, 127.7, 125.7, 124.8, 124.4, 123.2, 115.6, 47.8, 31.7, 29.2, 29.1, 26.8, 26.6, 22.6, 14.1. Anal. Calcd for $C_{30}H_{29}NO_2S_3$: C, 67.76; H, 5.50; N, 2.63. Found: C, 67.69; H, 5.59; N, 2.72. IR: cm^{-1} 2924, 2851, 1654, 1580, 1429, 1220, 1053, 792.

3,3'-(5,5'-(10-octyl-10*H*-phenothiazine-3,7-diyl)bis(thiophene-5,2-diyl))bis(2-cyanoacrylic acid) (PTZ2). **PTZ2** was synthetized according to general procedure C for Knoevenagel condensation using product **2** (140 mg, 0.26 mmol), cyanoacetic acid (220 mg, 2.6 mmol), piperidine (270 mg, 3.16 mmol) and $CHCl_3$ (5 mL). A dark red solid (150 mg) has been isolated as the product with 87 % of yield. ^{1}H NMR (500 MHz, DMSO): δ 8.48 (s, 2H), 8.00 (d, *J* = 4.2 Hz, 2H), 7.72 (d, *J* = 4.0 Hz, 2H), 7.64 – 7.56 (m, 4H), 7.14 (d, *J* = 8.4 Hz, 2H), 3.95 (t, *J* = 6.7 Hz, 2H), 1.76 – 1.62 (m, 2H), 1.45 – 1.37 (m, 2H), 1.34 – 1.16 (m, 8H), 0.82 (t, *J* = 6.7 Hz, 3H). ^{13}C NMR (126 MHz, DMSO): δ 164.1, 152.3, 147.0, 145.2, 142.0, 134.4, 127.6, 126.6, 125.0, 124.9, 124.0, 117.1, 117.0, 98.4, 63.3, 44.2, 31.5, 29.1, 28.9, 22.7, 22.5, 14.4. Anal. Calcd $C_{36}H_{31}N_3O_4S_3$: C, 64.94; H, 4.69; N, 6.31. Found: C, 64.71; H, 5.13; N, 6.26. IR: cm^{-1} 2921, 2846, 2218, 1678, 1559, 1479, 1393, 1355, 1250, 1212, 1061, 788.

10-octyl-3,7-di(thieno[3,2-b]thiophen-2-yl)-10*H*-phenothiazine (3a). Product **3a** was synthetized according to general procedure A for Suzuki-Miyaura cross-coupling using product **1** (500 mg, 1.07 mmol), Pd(dppf)Cl_2·CH_2Cl_2 (90 mg, 0.107 mmol), 4,4,5,5-tetramethyl-2-(thieno(3,2-b)thiophen-2-yl)-1,3,2-dioxaborolane (660 mg, 2.46 mmol), K_2CO_3 (1.50 g, 10.7 mmol), DME (7 mL) and methanol (7 mL). Extractions with AcOEt and purification with PE:DCM - 8:1 as eluent gave product **3a** as a yellow solid with a 84 % yield (530 mg). ^{1}H NMR (500 MHz, $CDCl_3$): δ 7.39 – 7.34 (m, 6H), 7.33 (d, *J* = 5.2 Hz, 2H), 7.23 (d, *J* = 5.2 Hz, 2H), 6.81 (d, *J* = 9.1 Hz, 2H), 3.81 (t, *J* = 7.2 Hz, 2H), 1.85 – 1.76 (m, 2H), 1.48 – 1.39 (m, 2H), 1.38 – 1.21 (m, 8H), 0.90 (t, *J* = 6.9 Hz, 3H). ^{13}C NMR (126 MHz, $CDCl_3$): δ 145.3, 144.2, 140.1, 138.0, 129.4, 126.5, 124.9, 124.6, 124.5, 119.6, 115.5, 114.4, 47.6, 31.8, 29.3, 29.2, 26.9, 26.8, 22.7, 14.2. Anal. Calcd for $C_{32}H_{29}NS_5$: C, 65.37; H, 4.97; N, 2.38. Found: C, 65.35; H, 4.83; N, 2.54. IR: cm^{-1} 2923, 2849, 1467, 1451, 1329, 1243, 1155, 807.

5,5'-(10-octyl-10*H*-phenothiazine-3,7-diyl)dithieno[3,2-b]thiophene-2-carbaldehyde (3b). Distilled $POCl_3$ (250 mg, 1.63 mmol) was added dropwise to DMF (120 mg, 1.63 mmol) at -15 °C under N_2 atmosphere; at the end of the addition a white solid formed, that, after 60 minutes, was dissolved in DMF (15 mL). Product **3a** (320 mg, 0.54 mmol) was added and the mixture warmed at 80 °C for 8 h. Then a saturated solution of NaOAc (30 mL) was added dropwise and the mixture was extracted with DCM (3 x 50 mL), the organic phases were combined and dried. Purification through column chromatography on silica gel, with PE:AcOEt - 3:1 as eluent, gave the product **3b** as orange solid with a 65 % yield (225 mg, 0.35 mmol). ^{1}H NMR (500 MHz, $CDCl_3$): δ 9.93 (s, 2H), 7.88 (s, 2H), 7.44 – 7.39 (m, 4H), 7.37 (d, *J* = 2.1 Hz, 2H), 6.87 (d, *J* = 8.5 Hz, 2H), 3.87 (t, *J* = 7.2 Hz, 2H), 1.88 – 1.79 (m, 2H), 1.50 – 1.42 (m, 2H), 1.37 – 1.22 (m, 8H), 0.87 (t, *J* = 6.9 Hz, 3H). ^{13}C NMR (126 MHz, $CDCl_3$): δ 183.0, 151.8, 146.9, 145.0, 144.3, 137.7, 129.1, 128.5, 125.5, 124.8, 124.6, 115.7, 114.9, 47.8, 31.7, 29.2, 29.2, 26.8, 26.7, 22.6, 14.1. Anal. Calcd. For $C_{34}H_{29}NO_2S_5$: C, 63.42; H, 4.54; N, 2.18. Found: C, 63.41; H, 4.50; N, 1.83. IR: cm^{-1} 2875, 1565, 1498, 1452, 1351, 1201, 1100, 1027, 920, 854, 729.

3,3'-(5,5'-(10-octyl-10*H*-phenothiazine-3,7-diyl)bis(thieno[3,2-b]thiophene-5,2-diyl))bis(2-cyanoacrylic acid) (PTZ3). PTZ3 was synthetized according to general procedure C for Knoevenagel condensation using product **3b** (200 mg, 0.31 mmol), cyanoacetic acid (270 mg, 3.10 mmol), piperidine (320 mg, 3.70 mmol) and $CHCl_3$ (10 mL). A dark red solid (200 mg) has been isolated as the product with a 83 % of yield. ^{1}H NMR

(500 MHz, DMSO): δ 8.55 (s, 2H), 8.29 (s, 2H), 7.96 (s, 2H), 7.63 – 7.44 (m, 4H), 7.10 (d, *J* = 8.4 Hz, 2H), 4.05 – 3.72 (m, 2H), 1.78 – 1.59 (m, 2H), 1.50 – 1.32 (m, 2H), 1.32 – 1.10 (m, 8H), 0.82 (t, *J* = 9.7 Hz, 3H).^{13}C NMR (126 MHz, DMSO): δ 164.2, 151.6, 147.9, 147.8, 144.8, 137.9, 137.1, 132.8, 128.4, 126.1, 124.5, 123.8, 117.0, 116.8, 116.5, 98.0, 63.3, 31.6, 29.1, 28.9, 26.5, 22.5, 14.4. Anal. Calcd. For $C_{40}H_{31}N_3O_4S_5$: C, 61.75; H, 4.02; N, 5.40. Found: C, 61.59; H, 4.29; N, 5.81. IR: cm^{-1} 2920, 2850, 2216, 1678, 1565, 1454, 1396, 1236, 1158, 1132, 796.

10-octyl-3,7-bis(4,4,5,5-tetramethyl-1,3,2-dioxaborolan-2-yl)-10*H*-phenothiazine (4). Product **1** (1.00 g, 2.14 mmol) was dissolved in THF (30 mL) under inert atmosphere and the solution cooled down to -78 °C. *n*-BuLi (1.6 M solution in hexane, 3.4 mL, 5.36 mmol) was then added dropwise and the mixture was left under magnetic stirring for 60 min. Then 2-isopropoxy-4,4,5,5-tetramethyl-1,3,2-dioxaborolane (1.00 g, 5.36 mmol) was added at -78 °C and the mixture was left under magnetic stirring for 48 h at rt. The quench was performed by pouring into 50 mL of a saturated solution of NH_4Cl and extractions with Et_2O were performed, followed by anhydrification. The crude product was a sticky liquid that was used for cross-coupling step without any further purification. ^{1}H NMR (500 MHz, $CDCl_3$): δ 7.55 (dd, *J* = 8.1, 1.3 Hz, 2H), 7.51 (d, *J* = 1.3 Hz, 2H), 6.80 (d, *J* = 8.2 Hz, 2H), 3.84 (t, *J* = 7.2 Hz, 2H), 1.81 – 1.73 (m, 2H), 1.42 – 1.35 (m, 2H), 1.31 (s, 24H), 1.28 – 1.19 (m, 8H), 0.88 (t, *J* = 7.2 Hz, 3H).

5',5'''-(10-octyl-10H-phenothiazine-3,7-diyl)bis((2,2'-bithiophene)-5-carbaldehyde) (5a). Product **5a** was synthetized according to general procedure B for Suzuki-Miyaura cross-coupling using product **4** (115 mg, 0.20 mmol), $Pd(dppf)Cl_2{\cdot}CH_2Cl_2$ (17 mg, 0.020 mmol), 5'-bromo-(2,2'-bithiophene)-5-carbaldehyde (120 mg, 0.44 mmol), K_2CO_3 (280mg, 2.0 mmol), DME (3 mL) and methanol (3 mL). Extractions with AcOEt and purification with DCM as eluent, gave product **5a** as an orange solid with a 64 % yield 90 mg). ^{1}H NMR (500 MHz, $CDCl_3$): δ 9.86 (s, 2H), 7.67 (d, *J* = 4.0 Hz, 2H), 7.39 (dd, *J* = 8.4, 2.2 Hz, 2H), 7.36 (d, *J* = 2.1 Hz, 2H), 7.31 (d, *J* = 3.8 Hz, 2H), 7.25 (d, *J* = 3.9 Hz, 2H), 7.17 (d, *J* = 3.8 Hz, 2H), 6.86 (d, *J* = 8.5 Hz, 2H), 3.87 (t, *J* = 7.2 Hz, 2H), 1.93 – 1.73 (m, 2H), 1.48 – 1.40 (m, 2H), 1.40 – 1.17 (m, 8H), 0.87 (t, *J* = 6.9 Hz, 3H).^{13}C NMR (126 MHz, $CDCl_3$): δ 182.4, 147.2, 145.1, 144.5, 141.5, 137.3, 134.4, 128.2, 127.2, 125.0, 124.7, 124.5, 123.8, 123.4, 115.6, 47.8, 31.7, 29.2, 26.9, 26.8, 22.6, 14.0. Anal. Calcd. For $C_{38}H_{33}NO_2S_5$: C, 65.58; H, 4.78; N, 2.01. Found: C, 65.38; H, 4.51; N, 1.28. IR: cm^{-1} 2920, 2851, 1649, 1442, 1367, 1223, 1047, 791.

3,3'-(5',5'''-(10-octyl-10*H*-phenothiazine-3,7-diyl)bis([2,2'-bithiophene]-5',5-diyl))bis(2-cyanoacrylic acid) (PTZ4). PTZ4 was synthetized according to general procedure C for Knoevenagel condensation using product **5a** (60 mg, 0.086 mmol), cyanoacetic acid (75 mg, 0.86 mmol), piperidine (100 mg, 1.04 mmol) and $CHCl_3$ (3 mL). A dark red solid (60 mg) has been isolated as the product with a 86 % of yield. ^{1}H NMR (500 MHz, DMSO): δ 8.46 (s, 2H), 7.97 (d, *J* = 4.1 Hz, 2H), 7.61 (d, *J* = 3.9 Hz, 2H), 7.58 (d, *J* = 3.9 Hz, 2H), 7.57 – 7.50 (m, 6H), 7.06 (d, *J* = 8.3 Hz, 2H), 3.92 (t, *J* = 6.5 Hz, 2H), 1.75 – 1.60 (m, 2H), 1.45 – 1.35 (m, 2H), 1.33 – 1.06 (m, 8H), 0.82 (t, *J* = 6.6 Hz, 3H). ^{13}C NMR (126 MHz, $CDCl_3$): δ 164.9, 147.3, 147.2, 146.8, 145.7, 145.3, 142.6, 135.3, 134.7, 129.7, 128.8, 126.5, 126.1, 125.1, 124.9, 118.1, 117.6, 99.9, 32.4, 30.0, 29.8, 27.4, 27.3, 23.6, 23.4, 15.3. Anal. Calcd. For $6C_{38}H_{33}NO_2S_5{\cdot}H_2O$: C, 63.41; H, 4.64; N, 5.04. Found: C, 62.81; H, 4.87; N, 5.35. IR: cm^{-1} 2925, 2215, 1686, 1570, 1400, 1254, 1207, 1155, 1052, 788.

5-bromo-3,4-dibutoxythiophene-2-carbaldehyde. 3,4-dibutoxythiophene (1.25 g, 5.47 mmol) was solubilized in dry THF (30 mL) under nitrogen atmosphere. The mixture was cooled to -78 °C and *n*-BuLi (3.76 mL, 6.02 mmol) was added dropwise. After having stirred the mixture for 60 min, DMF (480 mg, 6.57 mmol) was added and the mixture was stirred at rt for 15 h. Then the solvent was evaporated and the mixture was quenched with 50 mL of a saturated solution of NH_4Cl**,** extracted with Et_2O (3x50 mL), and dried. The isolated product (850 mg, 3.32 mmol) was solubilized in DMF (7 mL), temperature was lowered to -5 °C and NBS (710 mg, 3.97 mmol) was added dropwise as DMF solution (7 mL). The color changed from yellow to brown-green. After 7 h of stirring at rt, 50 mL of water were added and Et_2O extractions performed (3x50 mL). Anhydrification and purification through column chromatography (mixture of PE:AcOEt – 10:1 as eluent) allowed isolating the desired product (1.06 g, 3.16 mmol) as yellow oil with an overall yield of 58 %. The product has been used without any further purification for the following step. ^{1}H NMR (500 MHz, $CDCl_3$): δ 9.85 (s, 1H), 4.27 (t, *J* = 6.5 Hz, 2H), 4.03 (t, *J* = 6.5 Hz, 2H), 1.78 – 1.67 (m, 4H), 1.52 – 1.42 (m, 4H), 1.00 – 0.90 (m, 6H). ^{13}C NMR (126 MHz, $CDCl_3$): δ 180.0, 155.7, 147.5, 124.3, 112.1, 74.5, 73.9, 31.9, 31.8, 19.0, 18.9, 13.7, 13.6.

5,5'-(10-octyl-10*H*-phenothiazine-3,7-diyl)bis(3,4-dibutoxythiophene-2-carbaldehyde) (5b). Product **5b** was synthetized according to general procedure B for Suzuki-Miyaura cross-coupling using product **4** (200 mg, 0.35 mmol), $Pd(dppf)Cl_2{\cdot}CH_2Cl_2$ (30 mg, 0.035 mmol), 5-bromo-3,4-dibutoxythiophene-2-carbaldehyde (200 mg, 0.71 mmol), K_2CO_3 (500mg, 3.5 mmol), DME (5 mL) and methanol (5 mL). Purification with PE:AcOEt - 10:1 as eluent gave product **5b** as an orange solid with a 45 % yield (130 mg). ^{1}H NMR (500 MHz, $CDCl_3$): δ 9.98 (s, 2H), 7.61 (d, *J* = 2.1 Hz, 2H), 7.53 (dd, *J* = 8.6, 2.1 Hz, 2H), 6.85 (d, *J* = 8.6 Hz, 2H), 4.34 (t, *J* = 6.5 Hz, 4H), 3.91 (t, *J* = 6.5 Hz, 4H), 3.87 (t, *J* = 7.2,2H), 1.87 – 1.76 (m, 6H), 1.72 – 1.63 (m, 4H), 1.57 – 1.41 (m, 10H), 1.38 – 1.20 (m, 8H), 1.00 (t, *J* = 7.4 Hz, 6H), 0.94 (t, *J* = 7.4 Hz, 6H), 0.87 (t, *J* = 6.9 Hz, 3H). ^{13}C NMR (126 MHz, $CDCl_3$): δ 180.7, 157.4, 144.9, 144.7, 136.3, 126.7, 126.4, 125.9, 124.3, 121.3, 115.3, 74.5, 73.3, 47.8, 32.1, 32.0, 31.7, 29.2, 29.1, 26.8, 26.7, 22.6, 19.2, 19.0, 14.0, 13.8, 13.8. Anal. Calcd. For $C_{46}H_{61}NO_6S_3$: C, 67.36; H, 7.50; N, 1.71. Found: C, 67.69; H, 7.23; N, 2.00. IR: cm^{-1} 2956, 2927, 2871, 1647, 1578, 1459, 1417, 1401, 1350, 1254, 1105, 1062, 1029, 811.

3,3'-(5,5'-(10-octyl-10*H*-phenothiazine-3,7-diyl)bis(3,4-dibutoxythiophene-5,2-diyl))bis(2-cyanoacrylic acid) (PTZ5). PTZ5 was synthetized according to general procedure C for Knoevenagel condensation using product **5b** (200 mg, 0.23 mmol), cyanoacetic acid (200 mg, 2.32 mmol), piperidine (240 mg, 2.79 mmol) and $CHCl_3$ (10 mL). A dark red solid (200 mg) has been isolated as the product with a 90 % of yield. ^{1}H NMR (500 MHz, DMSO): δ 8.26 (s, 2H), 7.59 – 7.47 (m, 4H), 7.16 – 7.02 (m, 2H), 4.28 (t, *J* = 6.4 Hz, 6H), 3.95 – 3.85 (m, 8H), 1.78 – 1.67 (m, 6H), 1.67 – 1.55 (m, 4H), 1.52 – 1.44 (m, 4H), 1.44 – 1.35 (m, 6H), 1.32 – 1.15 (m, 8H), 0.95 (t, *J* = 7.4 Hz, 6H), 0.87 (t, *J* = 7.4 Hz, 6H), 0.82 (t, *J* = 6.8 Hz, 3H). ^{13}C NMR (126 MHz, DMSO): δ 164.2, 157.1, 145.4, 144.9, 141.4, 134.6, 127.0, 126.2, 125.5, 123.5, 117.1, 116.8, 116.0, 96.2, 74.4, 73.4, 31.9, 31.5, 29.0, 28.9, 26.4, 22.5, 19.2, 19.0, 14.4, 14.0. Anal. Calcd. For

$C_{52}H_{63}N_3O_8S_3$: C, 65.45; H, 6.65; N, 4.40. Found: C, 65.85; H, 6.06; N, 4.96. IR: cm^{-1} 2927, 2871, 2214, 1683, 1555, 1457, 1394, 1362, 1230, 1172, 1027, 794.

7,7'-(10-octyl-10H-phenothiazine-3,7-diyl)bis(2,3-dihydrothieno[3,4-b][1,4]dioxine-5-carbaldehyde) (5c). Product **5c** was synthetized according to general procedure B for Suzuki-Miyaura cross-coupling using product **4** (400 mg, 0.71 mmol), Pd(dppf)Cl_2·CH_2Cl_2 (58 mg, 0.071 mmol), 7-bromo-2,3-dihydrothieno[3,4-b][1,4]dioxine-5-carbaldehyde (400 mg, 1.56 mmol), K_2CO_3 (1.00 g, 7.10 mmol), DME (7 mL) and methanol (7 mL). Purification with DCM:Et_2O – 100:1 as eluent gave product **5c** as an orange solid with a 40 % yield (185 mg). ^{1}H NMR (500 MHz, $CDCl_3$): δ 9.90 (s, 2H), 7.57 (d, *J* = 2.1 Hz, 2H), 7.52 (dd, *J* = 8.6, 2.2 Hz, 2H), 6.82 (d, *J* = 8.6 Hz, 2H), 4.44 – 4.35 (m, 8H), 3.83 (t, *J* = 7.0 Hz, 2H), 1.80 – 1.75 (m, 2H), 1.47 – 1.06 (m, 10H), 0.86 (t, *J* = 6.5 Hz, 3H). ^{13}C NMR (126 MHz, $CDCl_3$): δ 179.4, 149.0, 144.6, 137.2, 128.0, 126.4, 126.0, 125.5, 124.1, 115.3, 115.0, 65.1, 64.5, 47.7, 31.7, 29.2, 29.1, 26.8, 26.7, 22.6, 14.1. Anal. Calcd. For $C_{34}H_{33}NO_6S_3$: C, 63.04; H, 5.13; N, 2.16. Found: C, 63.12; H, 4.96; N, 2.40. IR: cm^{-1} 2926, 2851, 1638, 1438, 1357, 1254, 1217, 1080, 805.

3,3'-(7,7'-(10-octyl-10*H*-phenothiazine-3,7-diyl)bis(2,3-dihydrothieno[3,4-b][1,4]dioxine-7,5-diyl))bis(2-cyanoacrylic acid) (PTZ6). PTZ6 was synthetized according to general procedure C for Knoevenagel condensation using product 5c (90 mg, 0.14 mmol), cyanoacetic acid (120 mg, 1.40 mmol), piperidine (140 mg, 1.67 mmol) and $CHCl_3$ (5 mL). A dark red solid (88 mg) has been isolated as the product with a 80 % of yield. ^{1}H NMR (500 MHz, DMSO): δ 8.14 (s, 2H), 7.48 (dd, *J* = 8.6, 1.7 Hz, 2H), 7.41 (d, *J* = 1.9 Hz, 2H), 6.97 (d, *J* = 8.8 Hz, 2H), 4.60 – 4.30 (m, 8H), 3.90 – 3.60 (m, 2H), 1.70 – 1.60 (m, 2H), 1.45 – 1.14 (m, 10H), 0.82 (t, *J* = 6.7 Hz, 3H). ^{13}C NMR (126 MHz, DMSO): δ 164.5, 149.6, 144.2, 140.2, 138.2, 126.6, 126.2, 126.1, 124.9, 123.0, 117.5, 116.4, 108.8, 94.4, 66.1, 65.2, 47.4, 31.6, 29.1, 29.0, 26.5, 26.3, 22.5, 14.4. Anal. Calcd. For $C_{40}H_{35}N_3O_8S_3$: C, 61.44; H, 4.51; N, 5.37. Found: C, 61.48; H, 4.77; N, 5.47. IR: cm^{-1} 2924, 2210, 1676, 1561, 1545, 1438, 1396, 1356, 1225, 1069, 1024, 760.

Acknowledgements

AA, BC, and NM thank the Ministero dell'Università e della Ricerca (MIUR-PRIN) (grant number 2008CSNZFR) for financial support. TM, IRO and PF acknowledge Prof. Juan José Delgado Jaén (University of Cadiz) for help and discussion on TEM analysis, the Ministero dell'Istruzione, Università e Ricerca (Project 2010N3T9M4 "HI-PHUTURE"), University of Trieste (FRA2013 Project) and University of Cadiz for access to TEM facilities.

Keywords: hydrogen production • photocatalysis • dyes stability • visible light • solar cells

[1] N. Armaroli, V. Balzani, *Energy for a Sustainable World: From the Oil Age to a Sun-Powered Future*, Wiley-VCH Verlag GmbH & Co. KGaA, **2010**.
[2]. www.iea.org
[3] B. O'Regan, M. Grätzel, *Nature*, **1991**, *353*, 737–740.
[4] A. Hagfeldt, G. Boschloo, L. Sun, L. Kloo, H. Pettersson, *Chem. Rev.*, **2010**, *110*, 6595–6663.
[5] A. Fujishima, K. Honda, *Nature*, **1972**, *238*, 37–38.
[6] M. Cargnello, A. Gasparotto, V. Gombac, T. Montini, D. Barreca, P. Fornasiero, *Eur. J. Inorg. Chem.*, **2011**, *2011*, 4309–4323.
[7] Z. Yu, F. Li, L. Sun, *Energy Environ. Sci.*, **2015**, *8*, 760–775.
[8] V. Balzani, A. Credi, M. Venturi, *ChemSusChem*, **2008**, *1*, 26–58.
[9] S. Zhang, X. Yang, Y. Numata, L. Han, *Energy Environ. Sci.*, **2013**, *6*, 1443–1464.
[10] Y.-S. Yen, H.-H. Chou, Y.-C. Chen, C.-Y. Hsu, J. T. Lin, *J. Mater. Chem.*, **2012**, *22*, 8734–8747.
[11] E. Bae, W. Choi, J. Park, H. S. Shin, S. Bin Kim, J. S. Lee, *J. Phys. Chem. B*, **2004**, *108*, 14093–14101.
[12] E. Reisner, D. J. Powell, C. Cavazza, J. C. Fontecilla-Camps, F. A. Armstrong, *J. Am. Chem. Soc.*, **2009**, *131*, 18457–18466.
[13] L. Yu, X. Zhang, C. Zhuang, L. Lin, R. Li, T. Peng, *Phys. Chem. Chem. Phys.*, **2014**, *16*, 4106–4114.
[14] S.-H. Lee, Y. Park, K.-R. Wee, H.-J. Son, D. W. Cho, C. Pac, W. Choi, S. O. Kang, *Org. Lett.*, **2010**, *12*, 460–463.
[15] R. Abe, K. Shinmei, N. Koumura, K. Hara, B. Ohtani, *J. Am. Chem. Soc.*, **2013**, *135*, 16872–16884.
[16] X. Li, S. Cui, D. Wang, Y. Zhou, H. Zhou, Y. Hu, J.-G. Liu, Y. Long, W. Wu, J. Hua, H. Tian, *ChemSusChem*, **2014**, *7*, 2879–2888.
[17] K. Kakiage, Y. Aoyama, T. Yano, T. Otsuka, T. Kyomen, M. Unno, M. Hanaya, *Chem. Commun.*, **2014**, *50*, 6379–6381.
[18] K. Kakiage, Y. Aoyama, T. Yano, K. Oya, T. Kyomen, M. Hanaya, *Chem. Commun.*, **2015**, *51*, 6315–6317.
[19] Z. Yao, M. Zhang, H. Wu, L. Yang, R. Li, P. Wang, *J. Am. Chem. Soc.*, **2015**, *137*, 3799–3802.
[20] A. Mishra, M. K. R. Fischer, P. Bäuerle, *Angew. Chemie Int. Ed.*, **2009**, *48*, 2474–2499.
[21] B.-G. Kim, K. Chung, J. Kim, *Chem. - A Eur. J.*, **2013**, *19*, 5220–5230.
[22] S. Ahmad, E. Guillén, L. Kavan, M. Grätzel, M. K. Nazeeruddin, *Energy Environ. Sci.*, **2013**, *6*, 3439–3466.
[23] M. Liang, J. Chen, *Chem. Soc. Rev.*, **2013**, *42*, 3453–3488.
[24] Y. Hua, S. Chang, D. Huang, X. Zhou, X. Zhu, J. Zhao, T. Chen, W.-Y. Wong, W.-K. Wong, *Chem. Mater.*, **2013**, *25*, 2146–2153.
[25] S. H. Kim, H. W. Kim, C. Sakong, J. Namgoong, S. W. Park, M. J. Ko, C. H. Lee, W. I. Lee, J. P. Kim, *Org. Lett.*, **2011**, *13*, 5784–5787.
[26] M. Cheng, X. Yang, J. Zhao, C. Chen, Q. Tan, F. Zhang, L. Sun, *ChemSusChem*, **2013**, *6*, 2322–2329.
[27] W.-I. Hung, Y.-Y. Liao, C.-Y. Hsu, H.-H. Chou, T.-H. Lee, W.-S. Kao, J. T. Lin, *Chem. Asian J.*, **2014**, *9*, 357–366.
[28] J. Lee, J. Kwak, K. C. Ko, J. H. Park, J. H. Ko, N. Park, E. Kim, D. H. Ryu, T. K. Ahn, J. Y. Lee, S. U. Son, *Chem. Commun.*, **2012**, *48*, 11431–11433.
[29] M. Watanabe, H. Hagiwara, A. Iribe, Y. Ogata, K. Shiomi, A. Staykov, S. Ida, K. Tanaka, T. Ishihara, *J. Mater. Chem. A*, **2014**, *2*, 12952–12961.
[30] N. Manfredi, B. Cecconi, A. Abbotto, *European J. Org. Chem.*, **2014**, *2014*, 7069–7086.
[31] A. Abbotto, N. Manfredi, C. Marinzi, F. De Angelis, E. Mosconi, J.-H. Yum, Z. Xianxi, M. K. Nazeeruddin, M. Grätzel, *Energy Environ. Sci.*, **2009**, *2*, 1094–1101.
[32] R. Y.-Y. Lin, F.-L. Wu, C.-H. Chang, H.-H. Chou, T.-M. Chuang, T.-C. Chu, C.-Y. Hsu, P.-W. Chen, K.-C. Ho, Y.-H. Lo, J. T. Lin, *J. Mater. Chem. A*, **2014**, *2*, 3092–3101.
[33] Z. Iqbal, W.-Q. Wu, H. Zhang, L. Han, X. Fang, L. Wang, D.-B. Kuang, H. Meier, D. Cao, *Org. Electron.*, **2013**, *14*, 2662–2672.
[34] I. D. L. Albert, T. J. Marks, M. A. Ratner, *J. Am. Chem. Soc.*, **1997**, *119*, 6575–6582.
[35] A. Albert, *Heterocyclic Chemistry*, Oxford University Press, New York, **1968**.
[36] A. Abbotto, N. Manfredi, *Dalt. Trans.*, **2011**, *40*, 12421–12438.
[37] W.-S. Han, K.-R. Wee, H.-Y. Kim, C. Pac, Y. Nabetani, D. Yamamoto, T. Shimada, H. Inoue, H. Choi, K. Cho, S. O. Kang, *Chem. - A Eur. J.*, **2012**, *18*, 15368–15381.
[38] J. Li, Y. E, L. Lian, W. Ma, *Int. J. Hydrogen Energy*, **2013**, *38*, 10746–10753.

[39] M. Sailer, A. W. Franz, T. J. J. Müller, *Chem. - A Eur. J.*, **2008**, *14*, 2602–2614.

[40] Z. B. Tang, X. X. Sun, P. L. Zhang, in *Advanced Materials Research*, **2014**, vol. 1061-1062, pp. 307–310.

[41] A. de Meijere, F. Diederich, *Metal-Catalyzed Cross-Coupling Reactions*, 2nd Edition, Wiley-VCH Verlag GmbH & Co. KGaA, **2008**.

[42] S. Alesi, F. Di Maria, M. Melucci, D. J. Macquarrie, R. Luque, G. Barbarella, *Green Chem.*, **2008**, *10*, 517–523.

[43] C.-Y. Kuo, Y.-C. Huang, C.-Y. Hsiow, Y.-W. Yang, C.-I. Huang, S.-P. Rwei, H.-L. Wang, L. Wang, *Macromolecules*, **2013**, *46*, 5985–5997.

[44] W.-H. Liu, I.-C. Wu, C.-H. Lai, C.-H. Lai, P.-T. Chou, Y.-T. Li, C.-L. Chen, Y.-Y. Hsu, Y. Chi, *Chem. Commun.*, **2008**, 5152–5154.

[45] N. Agarwal, S. P. Mishra, A. Kumar, C.-H. Hung, M. Ravikanth, *Chem. Commun.*, **2002**, 2642–2643.

[46] N. Agarwal, C.-H. Hung, M. Ravikanth, *Tetrahedron*, **2004**, *60*, 10671–10680.

[47] P. Chen, J. H. Yum, F. De Angelis, E. Mosconi, S. Fantacci, S.-J. Moon, R. H. Baker, J. Ko, M. K. Nazeeruddin, M. Grätzel, *Nano Lett.*, **2009**, *9*, 2487–2492.

[48] P. Docampo, S. Guldin, T. Leijtens, N. K. Noel, U. Steiner, H. J. Snaith, *Adv. Mater.*, **2014**, *26*, 4013–4030.

[49] J. Tauc, *Mater. Res. Bull.*, **1968**, *3*, 37–46.

[50] J. O. M. Bockris, S. U. M. Khan, *Surface Electrochemistry - A Molecular Level Approach*, Springer US, New York, **1993**.

[51] V. V Pavlishchuk, A. W. Addison, *Inorganica Chim. Acta*, **2000**, *298*, 97–102.

[52] F. Fabregat-Santiago, G. Garcia-Belmonte, I. Mora-Seró, J. Bisquert, *Phys. Chem. Chem. Phys.*, **2011**, *13*, 9083–9118.

[53] A. R. Katritsky, *Handbook of Heterocyclic Chemistry*, Pergamon Press, Oxford, **1983**.

[54] W. Zeng, Y. Cao, Y. Bai, Y. Wang, Y. Shi, M. Zhang, F. Wang, C. Pan, P. Wang, *Chem. Mater.*, **2010**, *22*, 1915–1925.

[55] X. Jiang, T. Marinado, E. Gabrielsson, D. P. Hagberg, L. Sun, A. Hagfeldt, *J. Phys. Chem. C*, **2010**, *114*, 2799–2805.

[56] E. M. Barea, C. Zafer, B. Gultekin, B. Aydin, S. Koyuncu, S. Icli, F. F. Santiago, J. Bisquert, *J. Phys. Chem. C*, **2010**, *114*, 19840–19848.

[57] W. H. Nguyen, C. D. Bailie, J. Burschka, T. Moehl, M. Grätzel, M. D. McGehee, A. Sellinger, *Chem. Mater.*, **2013**, *25*, 1519–1525.

[58] Y. Wu, X. Zhang, W. Li, Z.-S. Wang, H. Tian, W. Zhu, *Adv. Energy Mater.*, **2012**, *2*, 149–156.

[59] S. Qu, C. Qin, A. Islam, Y. Wu, W. Zhu, J. Hua, H. Tian, L. Han, *Chem. Commun.*, **2012**, *48*, 6972–6974.

[60] J. Liu, J. Zhang, M. Xu, D. Zhou, X. Jing, P. Wang, *Energy Environ. Sci.*, **2011**, *4*, 3021–3029.

[61] P. Ganesan, A. Chandiran, P. Gao, R. Rajalingam, M. Grätzel, M. K. Nazeeruddin, *J. Phys. Chem. C*, **2014**, *118*, 16896–16903.

[62] K. S. W. Sing, D. H. Everett, R. A. W. Haul, L. Moscou, R. A. Pierotti, J. Rouquerol, T. Siemieniewska, *Pure Appl Chem*, **1985**, *57*, 603–619.

[63] T. Montini, V. Gombac, L. Sordelli, J. J. Delgado, X. Chen, G. Adami, P. Fornasiero, *ChemCatChem*, **2011**, *3*, 574–577.

[64] I. Romero Ocaña, A. Beltram, J. J. Delgado Jaén, G. Adami, T. Montini, P. Fornasiero, *Inorganica Chim. Acta*, **2015**, *431*, 197–205.

[65] D. Y. C. Leung, X. Fu, C. Wang, M. Ni, M. K. H. Leung, X. Wang, X. Fu, *ChemSusChem*, **2010**, *3*, 681–694.

[66] X. Zhang, L. Yu, C. Zhuang, T. Peng, R. Li, X. Li, *RSC Adv.*, **2013**, *3*, 14363–14370.

[67] H. Kisch, D. Bahnemann, *J. Phys. Chem. Lett.*, **2015**, *6*, 1907–1910.

[68] S. Y. Reece, J. A. Hamel, K. Sung, T. D. Jarvi, A. J. Esswein, J. J. H. Pijpers, D. G. Nocera, *Science*, **2011**, *334*, 645–648.

[69] G. Carraro, C. Maccato, A. Gasparotto, T. Montini, S. Turner, O. I. Lebedev, V. Gombac, G. Adami, G. Van Tendeloo, D. Barreca, P. Fornasiero, *Adv. Funct. Mater.*, **2014**, *24*, 372–378.

[70] R. Abe, K. Shinmei, K. Hara, B. Ohtani, *Chem. Commun.*, **2009**, 3577–3579.

[71] P. Kumaresan, S. Vegiraju, Y. Ezhumalai, S. Yau, C. Kim, W.-H. Lee, M.-C. Chen, *Polymers (Basel).*, **2014**, *6*, 2645–2669.

[72] G. Zhang, Y. Bai, R. Li, D. Shi, S. Wenger, S. M. Zakeeruddin, M. Grätzel, P. Wang, *Energy Environ. Sci.*, **2009**, *2*, 92–95.

[73] M. Wang, M. Xu, D. Shi, R. Li, F. Gao, G. Zhang, Z. Yi, R. Humphry-Baker, P. Wang, S. M. Zakeeruddin, M. Grätzel, *Adv. Mater.*, **2008**, *20*, 4460–4463.

[74] J. Kim, H. Lee, D. Y. Kim, Y. Seo, *Adv. Mater.*, **2014**, *26*, 5191–5191.

[75] A. J. Bard, L. R. Faulkner, *Electrochemical Methods: Fundamentals and Applications*, 2nd edition, John Wiley & Sons Inc, **2001**.

[76] S. Ito, T. N. Murakami, P. Comte, P. Liska, C. Grätzel, M. K. Nazeeruddin, M. Grätzel, *Thin Solid Films*, **2008**, *516*, 4613–4619.

Entry for the Table of Contents (Please choose one layout)

Layout 1:

FULL PAPER

Dibranched D-(π-A)$_2$ thiophene-based phenothiazine dyes have been tested as photosensitizers in the photocatalytic production of hydrogen, in combination with a Pt/TiO_2 catalyst. In the hydrogen production over 20 h. the new sensitizers revealed improved stability after longer irradiation times and enhanced performances, in terms of hydrogen production rates and Light-to-Fuel efficiencies associated to enhanced stability.

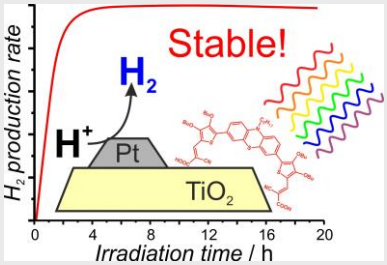

*Bianca Cecconi, Norberto Manfredi, Riccardo Ruffo, Tiziano Montini, Ismael Romero Ocaña, Paolo Fornasiero * and Alessandro Abbotto **

Page No. – Page No.

Tuning thiophene-based phenothiazines for stable photocatalytic H_2 production

Supporting Information

Click here to download Supporting Information: Cecconi Supporting Information.pdf